On time dependent and time independent vortex solutions

Kieran A. Arthur M.Sc.
6/8/96
PhD Thesis

School of Applied Mathematical Sciences
Dublin City University

Supervisor: Dr. J. Burzlaff.

I hereby certify that this material, which I now submit for assessment on the programme of study leading to the award of Doctor of Philosopy in Applied Mathematical Sciences is my own work and has not been taken from the work of others save and to the extent that such work has been cited and acknowledged within the text of my work.

Signed:

Kieran Arthur

Acknowledgements

I would like to thank my thesis advisor, Dr. Jűrgen Burzlaff, for his helpful comments, suggestions and criticisms throughout my research. I have enjoyed my time working with Dr. Burzlaff and I have learned a great deal from him.

I would like to thank Professor D.H. Tchrakian, St. Patrick's College Maynooth, with whom I worked. He suggested some problems that arose from our collaboration which now appear as chapters one through three in this dissertation. Professor Tchrakian encouraged me and was unfailingly optimistic that problems could be solved.

I would like to thank my family for their support and encouragement through the whole course of my studies, a period of time which may never have been envisaged when I started out nearly ten years ago.

I would like to thank, also, my fellow students, from whom I never ceased to learn. Some names, in particular come to mind, like those of Dr. K. Murphy, Mr. M. Ward, Mr F. Abdelwahid and Mr. S. Dowdall. I am left with very happy and sometimes strange memories of my time working with this great group of people. We must remember some friends who are no longer with us.

" For, lo, the winter is past
the rain is over and gone;
the flowers appear on the earth;
the time of the singing birds is come,
and the voice of the turtle is heard in the land. "

"Song of Solomon" [2:11-12]

Contents

List of Figures

List of Tables

Chapter 1

Introduction

The purpose of this thesis is to examine soliton-like solutions of various $2+1$ dimensional models, including the Ginzburg-Landau theory of superconductivity [1]. Among the models studied are also some with a Chern-Simons term, which may play a role in high temperature superconductivity [2]. Our study is relevant to planar physics and phenomena with cylindrical symmetry. Different models are studied to find generic features and pinpoint the differences. The most important property of the models we study is that there are extended structures in each of them. The models share many other properties which are investigated in this thesis.

The study of extended objects in gauge theories goes back to t'Hooft [3] and Polyakov [4] and their work on magnetic monopoles. Since then numerous papers have been written on static extended objects in gauge theories. In recent years the dynamics of soliton-like objects in $(2+1)$ and $(3+1)$ dimensions has also been studied. The analytic studies were mainly based on the geodesic approximation [5], whose validity has recently been proved for vortices [6] and monopoles [7], and were mainly concerned with the scattering of two objects. There are, however, some interesting analytic results for the scattering of more than two extended objects, (see for example Refs [8] [9] [10]). Our work will add to this body of knowledge.

In Chapters two to four various time independent solutions are exhibited and their interaction energies studied as a function of the relative strength of matter self coupling and electromagnetic coupling. The result is that the vortices have phases of attraction and repulsion. There is no interaction between the vortices when the topological lower bound on the energy is satu-

rated. Then vortices satisfy the corresponding first order partial differential equations. It will be shown that for the critical value of the coupling constant in the potential a lower bound on the energy of an $n-$vortex configuration can be attained. Since the vortex number is a topological invariant, any configuration which achieves this bound will be a minimum of the energy and thus a solution of the Euler-Lagrange equations.

Several models will be studied analytically and numerically in this way. In particular, in Chapter 3 the gauged $O(3)$ sigma model with Maxwell term and in Chapter 4 the gauged $O(3)$ sigma model with Chern-Simons term are studied. In Chapters 5 and 6 the Abelian Chern-Simons-Higgs vortices and the Abelian Yang-Mills-Higgs vortices are studied respectively. To find the static solutions a similar approach is taken, thus highlighting the generic features of the models.

The scattering properties of the vortices in the Abelian Yang-Mills-Higgs model are examined in the second half of this thesis. Given suitable initial data we prove that a global time dependent solution exists for the Abelian Higgs model. We show, using a formal method of solution to the equations, that symmetry properties of the initial data are retained by the solution. Considering transformations of the initial data which leave the energy density invariant, it is shown that the vortices scatter at a π/n angle.

When the vortices attain their minimal energy, the vortices do not interact and the diagonal components of the stress tensor vanish. Then the vortices can be placed at arbitrary positions in the plane. We exploit this fact to set up an initial value problem with initial boosts which does not cost any potential energy. The scattering properties can be examined for these processes.

Our aim is to study generic features of a whole range of vortex models, and to demonstrate how to progress from the statics to the dynamics of vortices in one of the models.

Chapter 2

The gauged O(3) sigma model with Maxwell term.

2.1 Introduction

Recently in Ref. [11] the $O(3)$ sigma model was gauged with a Maxwell $U(1)$ field. The self dual solutions of the model were examined, and it was shown that a soliton with $N = 1$ cannot exist. It is interesting to ask if the model supports attractive and repulsive phases. This analysis will be similar to that of Jacobs and Rebbi in Ref. [12] for the Abelian Higgs model and to that of Ref. [13] for Abelian Chern-Simons-Higgs vortices.

The Euler-Lagrange equations for the model will be found and solutions will be calculated numerically. Using these solutions, the energy will be evaluated as a function of the coupling constant, λ_0, of the potential. This measures the relative strength of matter self coupling and electromagnetic coupling. It will be seen that the vortices always repel.

2.2 The model

We start by defining the Lagrangian on $2+1$ dimensional Minkowski space, which is endowed with the metric $g = \text{diag}\,(+1, -1, -1)$,

$$\mathcal{L} = \frac{1}{2}(D_\mu \phi^a)(D^\mu \phi^a) - \frac{1}{4}F_{\mu\nu}F^{\mu\nu} - 2V(\phi^3). \tag{2.1}$$

Here the three component field $\vec{\phi}$ is constrained by $\phi^a\phi^a = 1$ with $a = 1, 2, 3$. The covariant derivative $D_\mu\phi^a$ is defined as,

$$D_\mu\phi^\alpha = \partial_\mu\phi^\alpha + A_\mu\varepsilon^{\alpha\beta}\phi^\beta, \qquad D_\mu\phi^3 = \partial_\mu\phi^3, \tag{2.2}$$

with $\alpha = 1, 2$. The gauge field is defined as, $F_{\mu\nu} = \partial_\mu A_\nu - \partial_\nu A_\mu$, with $\mu, \nu = 0, 1, 2$. The theories examined here will be gauge theories, that is models which exhibit invariance under gauge transformations.

The Lagrangian (2.1) is $U(1)$ gauge invariant. To see this we consider rotations about a fixed axis n, which is taken to be $n = (0, 0, 1)^T$. The rotations are of the form,

$$O(t, \vec{x}) = \begin{pmatrix} \cos\theta & \sin\theta & 0 \\ -\sin\theta & \cos\theta & 0 \\ 0 & 0 & 1 \end{pmatrix}, \tag{2.3}$$

where $\theta = \theta(t, \vec{x})$. The fields transform as,

$$\vec{\phi} \to \vec{\phi}' = O(t, \vec{x})\vec{\phi}, \tag{2.4}$$

and

$$A_\mu \to A'_\mu = A_\mu - \partial_\mu\theta. \tag{2.5}$$

Under this transformation the covariant derivative transforms as,

$$(D_\mu\vec{\phi})' = O(t, \vec{x})D_\mu\vec{\phi}. \tag{2.6}$$

The curvature $F_{\mu\nu} = \partial_\mu A_\nu - \partial_\nu A_\mu$, is invariant under this transformation.

The Euler-Lagrange equations of motion for the system are now calculated by including the term ,$\lambda((\phi^a)^2 - 1)$, in the Lagrangian to satisfy the constraint on the field $\vec{\phi}$. Variation with respect to the fields, A_ρ, ϕ^α and ϕ^3, respectively gives the following,

$$\partial_\mu F^{\rho\mu} = D^\rho\phi^\alpha\varepsilon^{\alpha\beta}\phi^\beta, \tag{2.7}$$

$$D_\rho D^\rho\phi^\alpha = 2\lambda\phi^\alpha, \tag{2.8}$$

$$\partial_\rho\partial^\rho\phi^3 - 2\frac{\partial}{\partial\phi^3}V = 2\lambda\phi^3. \tag{2.9}$$

Equations (2.8) and (2.9) can be combined to eliminate the Lagrange multiplier λ. Equation (2.8) is multiplied by ϕ^α and summed over α and equation

(2.9) is multiplied by ϕ^3 and the results are added. Using the constraint, we are left with the second Euler-Lagrange equation,

$$D_\rho D^\rho \phi^\alpha = (\phi^a D_\rho D^\rho \phi^a - 2\phi^3 \frac{\partial}{\partial \phi^3} V)\phi^\alpha. \tag{2.10}$$

The potential function, not yet specified, is allowed to depend only on the $U(1)$ invariant component ϕ^3 of $\vec{\phi}$.

From the energy momentum tensor of this Lagrangian a potential energy density will be found. If the Lagrangian does not depend explicitly on the coordinates x^ν, the derivative of the Lagrangian is given by,

$$\frac{\partial \mathcal{L}}{\partial x^\nu} = \frac{\partial \mathcal{L}}{\partial \eta_\rho} \frac{\partial \eta_\rho}{\partial x^\nu} + \frac{\partial \mathcal{L}}{\partial \eta_{\rho,\xi}} \frac{\partial \eta_{\rho,\xi}}{\partial x^\nu}. \tag{2.11}$$

When the Euler-Lagrange equations are substituted into the above, the result is

$$\frac{\partial \mathcal{L}}{\partial x^\nu} = \frac{\partial}{\partial x^\xi} \left(\frac{\partial \mathcal{L}}{\partial \eta_{\rho,\xi}} \eta_{\rho,\nu} \right) = \delta^\xi_\nu \frac{\partial \mathcal{L}}{\partial x^\xi}. \tag{2.12}$$

This equation can be written in terms of the divergence free quantity $\tilde{T}^\xi_\nu$,

$$\frac{\partial}{\partial x^\xi} \left(\frac{\partial \mathcal{L}}{\partial \eta_{\rho,\xi}} \eta_{\rho,\nu} - \delta^\xi_\nu \mathcal{L} \right) = \frac{\partial \tilde{T}^\xi_\nu}{\partial x^\xi} = 0. \tag{2.13}$$

The existence of a quantity, $\tilde{T}^\mu_\nu$, whose four divergence vanishes, is due to the fact that the Lagrangian has an explicit independence of the coordinates x_ν. The tensor $\tilde{T}^\mu_\nu$ is the energy momentum tensor of the field.

From this, the energy momentum tensor is defined by,

$$\tilde{T}^{\mu\nu} = \frac{\partial \mathcal{L}}{\partial \partial_\mu \eta_i} \partial^\nu \eta_i - g^{\mu\nu} \mathcal{L}. \tag{2.14}$$

When calculated it is,

$$\tilde{T}^{\mu\nu} = D^\mu \phi^\alpha \partial^\nu \phi^\alpha + \partial^\mu \phi^3 \partial^\nu \phi^3 - F^{\mu\rho} \partial^\nu A_\rho - g^{\mu\nu} \mathcal{L}. \tag{2.15}$$

The energy momentum tensor is defined only up to a four divergence, a fact which is used to symmetrise it,

$$\begin{aligned} T^{\mu\nu} &= \tilde{T}^{\mu\nu} + \partial_\rho (A^\nu F^{\mu\rho}) && (2.16) \\ &= \tilde{T}^{\mu\nu} + \partial_\rho A^\nu F^{\mu\rho} + A^\nu D^\mu \phi^\alpha \varepsilon^{\alpha\beta} \phi^\beta && (2.17) \\ &= D^\mu \phi^a D^\nu \phi^a - F^{\mu\rho} F^\nu{}_\rho - g^{\mu\nu} \mathcal{L}, && (2.18) \end{aligned}$$

where the second last line is found using the equation of motion.

The potential energy density is,

$$T_{00} = \mathcal{H}_0 = \frac{1}{2} D_i \phi^a D_i \phi^a + \frac{1}{4} F_{ij} F_{ij} + 2V. \tag{2.19}$$

The choice of potential function will be dictated by the requirement that the volume integral of this energy is bounded below by a topological number. This fixes the potential. To obtain finite energy configurations, for our choice of potential, we require,

$$\lim_{|x| \to \infty} \vec{\phi}(t, \vec{x}) = \vec{n}, \tag{2.20}$$

where $\vec{n}$ is some constant vector in internal space, that is the three dimensional field-space, whose components are labelled by a. Since $\vec{\phi}$ approaches the same value at all points at infinity, the physical coordinate space $\mathbf{R}^2$ can be mapped onto a sphere. The map is the stereographic projection. "It compactifies the space $\mathbf{R}^2$." The internal space is subject to the constraint, $(\phi^a)^2 - 1 = 0$, which is also a sphere. So any such finite energy static configuration is a mapping from one sphere to another.

Let S be the smooth surface defined parametrically by the one-to-one function $\vec{f}$ from $\mathbf{R}^2$ to $\mathbf{R}^3$ defined on a domain D in $\mathbf{R}^2$. Then $|\frac{\partial}{\partial u} \vec{f}(u_0, v_0)|$ is the length of a tangent vector to the curve given parametrically by $\vec{f}(u, v_0)$ at the point $\vec{f}(u_0, v_0)$. Similarly $|\frac{\partial}{\partial u} \vec{f}(u_0, v_0)|$ is the length of a tangent vector to the curve given parametrically by $\vec{f}(u_0, v)$ at the point $\vec{f}(u_0, v_0)$. The nonzero vector,

$$\frac{\partial}{\partial u} \vec{f}(u_0, v_0) \times \frac{\partial}{\partial v} \vec{f}(u_0, v_0) \tag{2.21}$$

defines a unique normal vector to the surface S at the point (u_0, v_0). The area of this parallelogram in the tangent plane to S is the absolute value of this, or

$$\langle \frac{\partial}{\partial u} \vec{f}(u_0, v_0) \times \frac{\partial}{\partial v} \vec{f}(u_0, v_0), \vec{n} \rangle \tag{2.22}$$

where $\vec{n}$ is a unit normal to S. The area of the surface is,

$$s = \int \int_D \langle \frac{\partial}{\partial u} \vec{f}(u_0, v_0) \times \frac{\partial}{\partial v} \vec{f}(u_0, v_0), \vec{n} \rangle du dv = \int_S ds \tag{2.23}$$

where the differential area element is,

$$ds = \langle \frac{\partial}{\partial u} \vec{f}(u_0, v_0) \times \frac{\partial}{\partial v} \vec{f}(u_0, v_0), \vec{n} \rangle du dv. \tag{2.24}$$

Using the above with $\vec{\phi}$ as a map from Cartesian coordinates to the coordinates of a sphere, we have the differential area element,

$$\varrho_0 = \varepsilon_{ij}\varepsilon^{abc}\partial_i\phi^a\partial_j\phi^b\phi^c. \tag{2.25}$$

We have chosen $\vec{\phi}$ as the unit normal vector. The integral of this quantity measures how many times the mapping $\vec{\phi}$ "covers" the sphere, that is the winding number,

$$Q = \frac{1}{8\pi}\int \varepsilon_{ij}\varepsilon^{abc}\partial_i\phi^a\partial_j\phi^b\phi^c d^2x. \tag{2.26}$$

This integral will provide a lower bound on the potential energy.

2.3 Self-dual solutions

The configurations which attain the lower bound of the potential energy are the self dual solutions. To explain the connection we make with the gauged version of the winding number density ϱ_0, which is,

$$\varrho_1 = \varepsilon_{ij}\varepsilon^{abc}D_i\phi^a D_j\phi^b\phi^c. \tag{2.27}$$

ϱ_1 is related to ϱ_0 as follows,

$$\varrho_1 = \varrho_0 + 2\varepsilon_{ij}\partial_i(\phi^3 A_j) - \varepsilon_{ij}\phi^3 F_{ij}, \tag{2.28}$$

which can be seen by expanding ϱ_1.

The occurrence of stable solutions, that is, solutions which attain a finite lower bound in energy, can be inferred from the following inequalities:

$$(\varepsilon_{ij}D_i\phi^a - \varepsilon^{abc}D_j\phi^b\phi^c)^2 \geq 0 \tag{2.29}$$

$$(D_i\phi^a)^2 \geq \varepsilon_{ij}\varepsilon^{abc}D_i\phi^a D_j\phi^b\phi^c = \varrho_1. \tag{2.30}$$

The other inequality is,

$$(\frac{1}{2}F_{ij} - \varepsilon_{ij}\sqrt{V})^2 \geq 0 \tag{2.31}$$

$$\frac{1}{4}F_{ij}^2 + 2V \geq \varepsilon_{ij}F_{ij}\sqrt{V}. \tag{2.32}$$

A lower bound on the potential energy density (2.19) can be obtained from the inequalities (2.30) and (2.32),

$$\begin{aligned}\mathcal{H}_0 = \frac{1}{4}F_{ij}^2 + \frac{1}{2}(D_i\phi^a)^2 + 2V &\geq \frac{1}{2}\varrho_0 + \varepsilon_{ij}\partial_i(\phi^3 A_j) - \frac{1}{2}\varepsilon_{ij}F_{ij}\phi^3 + \varepsilon_{ij}F_{ij}\sqrt{V} \\ &\geq \frac{1}{2}\varrho_0 + \varepsilon_{ij}\partial_i(\phi^3 A_j) - \frac{1}{2}\varepsilon_{ij}F_{ij}(\phi^3 - 2\sqrt{V})\end{aligned}$$

The lower bound can be arranged to be equal to one half the winding number density ϱ_0 plus a total divergence by choosing,

$$\sqrt{V} = \frac{1}{2}(\phi^3 - 1). \tag{2.33}$$

It follows from (2.28) then that the resulting inequality is,

$$\int d^2x\mathcal{H}_0 \geq \int d^2x \left(\frac{1}{2}\varrho_0 + \varepsilon_{ij}\partial_i(\phi^3 A_j) - \frac{1}{2}\varepsilon_{ij}F_{ij}\phi^3 + \varepsilon_{ij}F_{ij}\sqrt{V}\right). \tag{2.34}$$

When the potential is specified, the result is,

$$\begin{aligned}\int d^2x\mathcal{H}_0 &\geq \int d^2x \left(\frac{1}{2}\varrho_0 + \varepsilon_{ij}\partial_i(\phi^3 A_j - A_j)\right) \\ &= \frac{1}{2}\int d^2x\varrho_0 + \int dS_i\varepsilon_{ij}A_j(\phi^3 - 1),\end{aligned} \tag{2.35}$$

with $\mathcal{H}_0$ now given by

$$\mathcal{H}_0 = \frac{1}{4}F_{ij}^2 + \frac{1}{2}(D_i\phi^a)^2 + \frac{1}{2}(\phi^3 - 1)^2. \tag{2.36}$$

The requirement that the surface integral should vanish is satisfied by choosing appropriate boundary conditions. To ensure that the solutions have finite energy we choose,

$$\lim_{|\vec{x}|\to\infty} \phi^3 = 1. \tag{2.37}$$

With a stereographic projection in mind we also require,

$$\lim_{|\vec{x}|\to 0} \phi^3 = -1. \tag{2.38}$$

Conditions on the fields, A_i, will be found for our radial field configuration. The inequality (2.35) is saturated when the inequalities (2.30) and (2.32) are saturated, yielding the Bogomol'nyi equations,

$$F_{ij} = -\varepsilon_{ij}(1 - \phi^3), \tag{2.39}$$

$$\varepsilon_{ij} D_i \phi^a = \varepsilon^{abc} D_j \phi^b \phi^c. \tag{2.40}$$

Our radially symmetric Ansatz for the fields A_i and ϕ^a is,

$$A_i = \frac{a(r) - N}{r} \varepsilon_{ij} \hat{x}_j, \tag{2.41}$$

$$\phi^\alpha = \sin f(r)\, n^\alpha,\ \phi^3 = \cos f(r), \tag{2.42}$$

where $\hat{x}_i = \frac{x_i}{r}$ and $\vec{n} = (\cos N\theta, \sin N\theta)$ are unit vectors, with N an integer. A_0 is equal to zero.

The Bogomol'nyi equations (2.39) and (2.40) now reduce to the following pair of coupled nonlinear first order ordinary differential equations,

$$\frac{a'}{r} = -(1 - \cos f), \qquad f' = -\frac{a \sin f}{r}. \tag{2.43}$$

The boundary conditions now read,

$$\lim_{r \to 0} f(r) = \pi, \qquad \lim_{r \to \infty} f(r) = 0. \tag{2.44}$$

These conditions imply that for the Ansatz (2.41), (2.42), the winding number, Q, is equal to N. It should be noted that these boundary conditions are for the anti-self-dual field configurations, compared to Ref. [11]. This is the same as in the usual (ungauged) $O(3)$ model where the radially symmetric anti-self-dual vortices satisfy the asymptotic conditions (2.44) , while the self-dual vortices satisfy instead $\lim_{r \to 0} f(r) = 0$; $\lim_{r \to \infty} f(r) = \pi$.

Boundary conditions for the function $a(r)$ are found by requiring first that the fields A_i be regular at the origin,

$$\lim_{r \to 0} a(r) = N. \tag{2.45}$$

The constraint on the large r behaviour of $a(r)$ is, again, the requirement that the energy is finite. Since the energy density contains the term $\frac{a(r)^2}{r^2}$, we require that the derivative of $a(r)$ vanish as $r \to \infty$, or that,

$$\lim_{r \to \infty} a(r) = \alpha, \tag{2.46}$$

where α is a nonzero constant.

2.4 Non-self dual solutions

We will not study further the Bogomolny'i equations. It should be noted that in Ref. [11], the nonexistence of the $N = 1$ soliton has been demonstrated. We will examine solutions of the $O(3)$ model with potential,

$$V(\phi^3) = \frac{\lambda_0}{4}(\phi^3 - 1)^2, \tag{2.47}$$

where λ_0 is a positive constant not restricted to $\lambda_0 = 1$, which is the self-dual case. We will then study numerically solutions of vorticity $N = 2$ and $N = 3$.

Using the Ansatz (2.41), (2.42) the static Hamiltonian, (2.19), reduces to the one dimensional subsystem,

$$\mathcal{L} = \frac{r}{2}\left[\left(\frac{a_r}{r}\right)^2 + f_r^2 + \left(\frac{a\,\sin f}{r}\right)^2 + \lambda_0(1-\cos f)^2\right], \tag{2.48}$$

defined by,

$$\int d^2x\,\mathcal{H} = 2\pi \int dr\,\mathcal{L}. \tag{2.49}$$

In the potential the coupling constant, λ_0, appears; when this is equal to unity, the Bogomol'nyi equations can be imposed. When the one dimensional Lagrangian is varied the resulting equations are,

$$a(r)\sin^2 f(r) + \frac{a_r(r)}{r} - a_{rr}(r) = 0 \tag{2.50}$$

$$\lambda_0 r(1-\cos f(r))\sin f(r) + \frac{a^2\cos f\sin f}{r} - f_r - r f_{rr} = 0, \tag{2.51}$$

where $f_r = \frac{df}{dr}$. It is important to note that we could have substituted the Ansatz into the full Euler-Lagrange equations and obtained the same equations as above.

We first examine the equations (2.50) and (2.51) in the region $r \ll 1$ region. The power series solution is,

$$f(r) = \pi + f_o r^N + \frac{f_o(NA_o - \lambda_0)}{2(N+1)} r^{N+2} + O(r^{N+4}) \tag{2.52}$$

$$a(r) = N + A_o r^2 + \frac{f_o^2}{2(2N+2)} r^{2N+2} + O(r^{2N+4}). \tag{2.53}$$

The constants f_o and A_o are fixed by the asymptotic value of the solution at infinity. They are found by numerical methods, which require the correct values of the fields at the boundary. Using a power series solution of the Bogomol'nyi equations, it is found that the value of the constant A_o is fixed to be 1. This gives one free parameter in the power series which controls the behaviour of the solutions. It will also serve as a check on the numerically evaluated constants, in the one dimensional Euler-Lagrange equations, for the case where λ_0 is unity.

Now considering the region $r \gg 1$ and anticipating decaying solutions, we linearise the Euler Lagrange equations about their asymptotic values. That is, the equations are linearised in the functions $F(r)$ about $f = 0$ and $A(r)$ around the asymptotic value $a(r) = \alpha$. The Euler Lagrange equation for $f(r)$ linearised about its asymptotic value is,

$$\alpha^2 F - rF_r - r^2 F_{rr} = 0, \tag{2.54}$$

whose solution is,

$$F = \frac{c_1}{r^\alpha} + c_2 r^\alpha. \tag{2.55}$$

In order to have decaying solutions, the constant c_2 is chosen as zero. Here, $\alpha > 1$ must hold for the first term in (2.50) to be subdominant. The equation for $a(r)$ about its value is,

$$ra_{rr} - a_r = 0. \tag{2.56}$$

The solutions to this equation are $a = c_3 r^2$ or that a is a constant. The restriction to consideration of finite energy solutions, means that the behaviour of $\lim_{r\to\infty} a(r)$ =constant. This constant is chosen to be α. In the self dual case, a restriction is calculated from the Bogomol'nyi equations on the possible values of the constant, $\alpha > 1$.

2.5 Numerical Analysis

We have studied the equations numerically using a shooting method. The integration started in the region $r \ll 1$ using as initial data the power series solutions. The constants f_o and A_o have been found which give the correct asymptotic behaviour. The profiles for the functions $f(r)$ for vorticity $N = 2, 3$ and those for $a(r)$ are given in figures 1,2,4,5, and the respective

energy density profiles in figures 3 and 6. In table 3 the total energies of the vortices have been calculated for the approximate solutions. If the Bogomolny'i equations are substituted into the one dimensional system the result is,

$$\mathcal{L} = -a_r(1 - \cos f) - a f_r \sin f. \tag{2.57}$$

The total energy of a self dual solution can be written as,

$$\begin{aligned} E_{sd} &= -2\pi \int_0^\infty dr \left[a_r(1 - \cos f) + a f_r \sin f\right], && (2.58)\\ &= -2\pi \int_0^\infty dr \, \frac{d}{dr}\left(a(1 - \cos f)\right) && (2.59)\\ &= 4N\pi. && (2.60) \end{aligned}$$

This last line is found using the boundary conditions for both functions $a(r)$ and $f(r)$. The energy is independent of the choice of the number α. It is enough that $a_r = 0$ as $r \to \infty$. The figures of the energy density for the value of constant $\lambda_0 = 1$ is the self dual limit. It can be seen that the calculated values are close approximations to the analytic calculation. In figure 7, the values of the total energy are plotted. For the $N = 2$ vortex, these figures are multiplied by $\frac{3}{2}$. It can be seen that the $N = 2$ vortex energy is larger than the $N = 3$ energy. Only at the value of the constant $\lambda_0 = 1$ are the energies per unit vortex number equal. This means that all non-self-dual vortices attract. Two vortices are heavier per unit vorticity than a three vortex. The values of the constant A_o for the self dual solution should be unity. Again, the numerically calculated value is close.

Figure 2.1: Profile of the function $f(r)$ for the vortices with $N = 2$ with $\lambda_0 = 1.2, \ldots, 0.8$.

Figure 2.2: Profile of the function $a(r)$ for the vortices with $N = 2$ with lower values of α corresponding to lower λ_0.

Figure 2.3: Profile of the energy density for the $N = 2$ vortices where increasing peaks represent increasing energy and increasing λ_0.

Figure 2.4: Profile of the function $f(r)$ for the vortices with $N = 3$ with $\lambda_0 = 1.2, \ldots, 0.8$.

Figure 2.5: Profile of the function $a(r)$ for the vortices with $N = 3$ with lower values of α corresponding to lower λ_0.

Figure 2.6: Profile of the energy density for the $N = 3$ vortices where increasing peaks represent increasing energy and increasing λ_0.

Figure 2.7: Graph of the energy of two superimposed vortices, $E(\lambda_0, N = 2)/2$ and $E(\lambda_0, N = 3)/3$, as a function of λ_0.

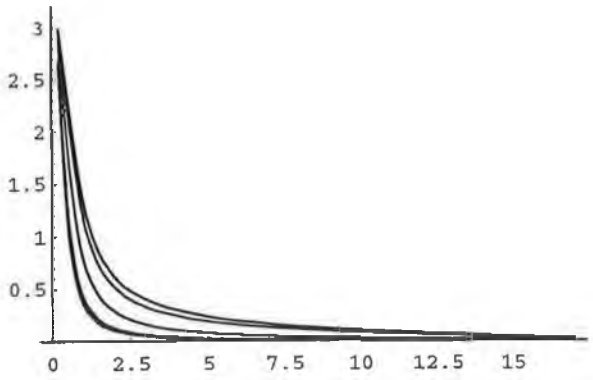

Figure 1

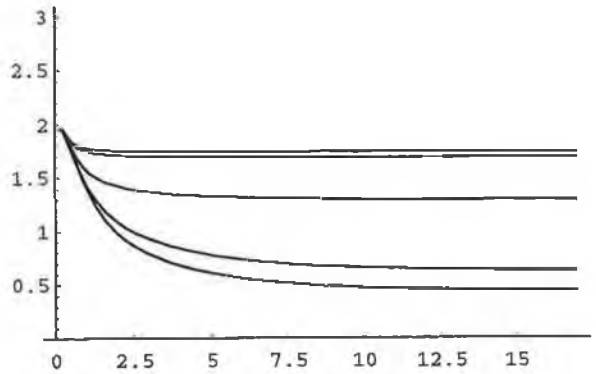

Figure 2

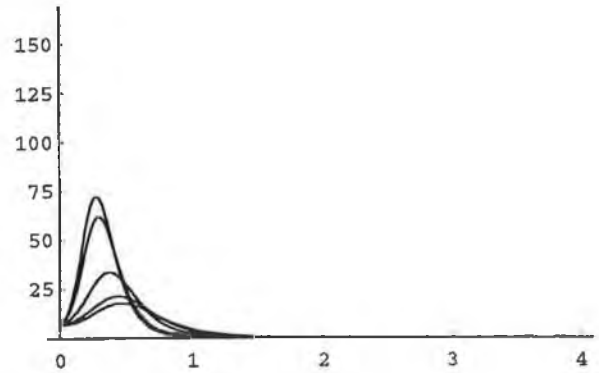

Figure 3

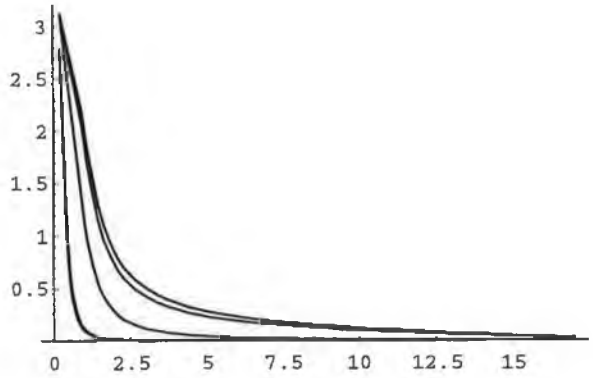

Figure 4

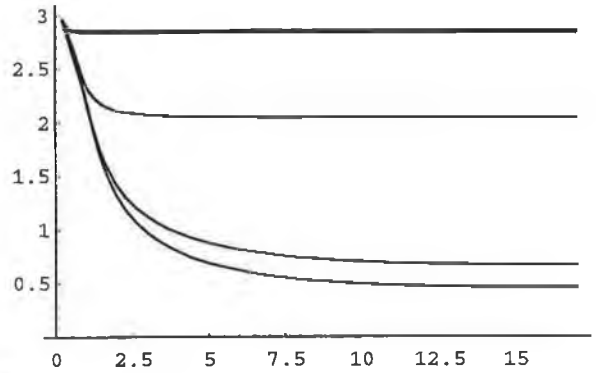

Figure 5

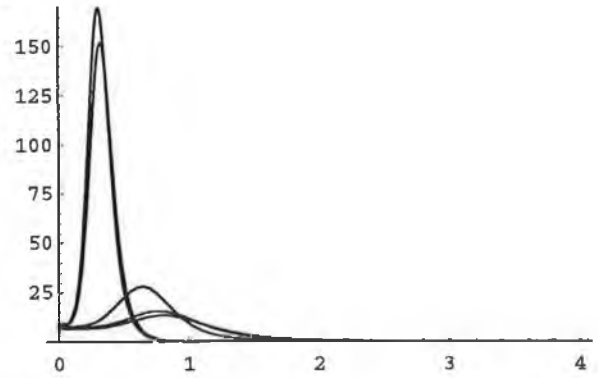

Figure 6

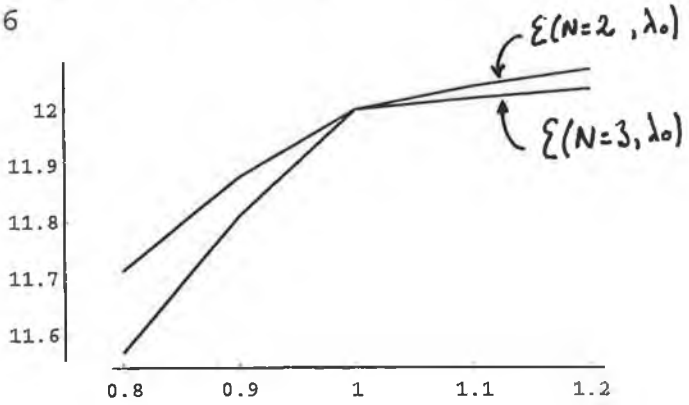

Figure 7

Constants	$N = 2$	
λ_0	A_o	f_o
0.8	-0.94596	-3.77798
0.9	-0.97511	-4.48613
1.0	-1.00040	-6.91181
1.1	-0.99567	-12.00442
1.2	-0.99375	-13.70814

Table 2.1: Numerically evaluated constants A_o and f_o for $N = 2$

Constants	$N = 3$	
λ_0	A_o	f_o
0.8	-0.93476	-2.00377
0.9	-0.96942	-2.40738
1.0	-1.00000	-5.00000
1.2	-0.99777	-51.79950

Table 2.2: Numerically evaluated constants A_o and f_o for $N = 3$

Constants	Energy	
λ_0	$E(N = 2, \lambda_0)$	$E(N = 3, \lambda_0)$
0.8	7.8087	11.5668
0.9	7.9189	11.8091
1.0	8.0004	11.9999
1.1	8.0281	12.0209
1.2	8.0481	12.0377

Table 2.3: Numerically evaluated energies for $N = 2, 3$ in units of π.

Chapter 3

The gauged O(3) sigma model with Chern-Simons term

3.1 Introduction

This chapter extends from work carried out in [14], [15] examining the self-dual vortices of the Chern-Simons O(3) gauged sigma model. We examine the non-self dual vortices and numerically evaluate the total energies of the static solutions. It is interesting to ask if the model supports attractive and repulsive phases. This analysis will be similar to that of the previous chapter and of the references therein.

3.2 The model

We start by defining the Lagrangian on $2+1$ dimensional Minkowski space,

$$\mathcal{L} = \frac{\kappa}{2}\varepsilon^{\mu\nu\rho}F_{\mu\nu}A_\rho + (D_\mu\phi^a)^2 - 4V(\phi^3), \tag{3.1}$$

where the three component field $\vec{\phi}$ is again constrained by $\phi^a\phi^a = 1$, and the covariant derivative $D_\mu\phi^a$ is defined as in the previous chapter, and with the opposite sign of the coupling used in [11], as

$$D_\mu\phi^\alpha = \partial_\mu\phi^\alpha + A_\mu\varepsilon^{\alpha\beta}\phi^\beta, \qquad D_\mu\phi^3 = \partial_\mu\phi^3. \tag{3.2}$$

The Lagrangian (3.1) changes by the total divergence,

$$-2\partial_\mu(\varepsilon^{\mu\nu\rho}A_\nu\partial_\rho\theta) \tag{3.3}$$

under the $U(1)$ transformation (2.4),(2.5), from the previous chapter, and any solution of the Euler-Lagrange equations is transformed to a new solution under that $U(1)$ gauge transformation. The potential function, not yet specified, is allowed to depend only on the $U(1)$ invariant component ϕ^3 of $\vec{\phi}$. The energy momentum tensor of this Lagrangian is, [15],

$$T_{\mu\nu} = 2D_\mu\phi^a D_\nu\phi^a - g_{\mu\nu}(D_\rho\phi^a D^\rho\phi^a - 4V) \tag{3.4}$$

The Hamiltonian density is given by,

$$T_{00} = \mathcal{H} = D_0\phi^a D_0\phi^a + D_i\phi^a D_i\phi^a + 4V. \tag{3.5}$$

The equation of motion given by the variation of A_ρ is,

$$\kappa\varepsilon^{\mu\nu\rho}F_{\mu\nu} + 2\varepsilon^{\alpha\beta}\phi^\beta D^\rho\phi^\alpha = 0. \tag{3.6}$$

One of these equations can be used to solve for A_0 and used to eliminate the time component of the gauge connection from the stress tensor density. The time component of equation (3.6) is,

$$\kappa\varepsilon^{ij}F_{ij} + 2\varepsilon^{\alpha\beta}\phi^\beta D_0\phi^\alpha = 0. \tag{3.7}$$

For static $\vec{\phi}$, this is solved for A_0 yielding,

$$A_0 = -\frac{\kappa}{2}\frac{\varepsilon^{ij}F_{ij}}{(\phi^\alpha)^2}. \tag{3.8}$$

In the static case, $T_{00} = \mathcal{H}$ then reduces to,

$$\begin{aligned}\mathcal{H}_0 &= A_0^2(\phi^\alpha)^2 + (D_i\phi^a)^2 + 4V \\ &= \frac{\kappa^2}{2}\frac{F_{ij}^2}{(\phi^\alpha)^2} + (D_i\phi^a)^2 + 4V\end{aligned}$$

The choice of potential function will again be dictated by the requirement that the volume integral of $\mathcal{H}$ is bounded below by a topological charge. This

fixes the potential. The usual winding number density $\varrho_0 = \varepsilon_{ij}\varepsilon^{abc}\partial_i\phi^a\partial_j\phi^b\phi^c$ is related to its gauged version,

$$\varrho_1 = \varepsilon_{ij}\varepsilon^{abc}D_i\phi^a D_j\phi^b\phi^c, \tag{3.9}$$

as we have seen in the previous chapter. The lower bound on the volume integral of the density (3.9) can be inferred from the following inequalities. First, as for the previous model, we use:

$$\begin{aligned}(\varepsilon_{ij}D_i\phi^a - \varepsilon^{abc}D_j\phi^b\phi^c)^2 &\geq 0 &(3.10)\\ (D_i\phi^a)^2 &\geq \varepsilon_{ij}\varepsilon^{abc}D_i\phi^a D_j\phi^b\phi^c = \varrho_1. &(3.11)\end{aligned}$$

The expression on the righthand side can be expanded,

$$(D_i\phi^a)^2 \geq \varrho_0 + 2\varepsilon_{ij}\partial_i(\phi^3 A_j) - \varepsilon_{ij}F_{ij}\phi^3. \tag{3.12}$$

The other inequality is,

$$\begin{aligned}(\frac{\kappa}{\sqrt{2}|\phi^\alpha|}F_{ij} - \sqrt{2}\varepsilon_{ij}|\phi^\alpha|U)^2 &\geq 0 &(3.13)\\ \left(\frac{\kappa^2}{2}\frac{F_{ij}^2}{|\phi^\alpha|^2} + 4U^2|\phi^\alpha|^2\right) &\geq 2\kappa\varepsilon_{ij}F_{ij}U. &(3.14)\end{aligned}$$

A lower bound on the potential energy density $\mathcal{H}_0$ can be deduced from the inequalities (3.12) and (3.14),

$$\begin{aligned}\mathcal{H}_0 &= \left[\frac{\kappa^2}{2}\frac{F_{ij}^2}{(\phi^\alpha)^2} + (D_i\phi^a)^2 + 4V\right] &(3.15)\\ &= \left[\frac{\kappa^2}{2}\frac{F_{ij}^2}{(\phi^\alpha)^2} + (D_i\phi^a)^2 + 4U^2|\phi^\alpha|^2\right] &(3.16)\\ &\geq \varrho_0 + 2\varepsilon_{ij}\partial_i(\phi^3 A_j) - \varepsilon_{ij}F_{ij}\phi^3 + 2\kappa\varepsilon_{ij}F_{ij}U &(3.17)\\ &= \varrho_0 + 2\varepsilon_{ij}\partial_i(\phi^3 A_j) - \varepsilon_{ij}F_{ij}(\phi^3 - 2\kappa U). &(3.18)\end{aligned}$$

The lower bound can be arranged to be equal to the winding number density $\frac{1}{2}\varrho_0$ plus a total divergence by identifying $U^2|\phi^\alpha|^2$ as the potential, and defining,

$$U = \frac{1}{2\kappa}(\phi^3 - 1). \tag{3.19}$$

So the potential is,

$$V = \frac{1}{4\kappa^2}(1-\phi^3)^3(1+\phi^3). \tag{3.20}$$

It follows that the resulting topological inequality is,

$$\begin{aligned}
\int d^2x\mathcal{H}_0 &\geq \int d^2x\varrho_0 + 2\int d^2x\varepsilon_{ij}\left(\partial_i(\phi^3 A_j) - \frac{1}{2}F_{ij}\right) && (3.21)\\
&\geq \int d^2x\varrho_0 + 2\int d^2x\partial_i\left(\varepsilon_{ij}A_j(\phi^3-1)\right) && (3.22)\\
&\geq \int d^2x\varrho_0 + 2\int dS_i\varepsilon_{ij}A_j(\phi^3-1), && (3.23)
\end{aligned}$$

with $\mathcal{H}_0$ now given by

$$\mathcal{H}_0 = \frac{\kappa^2}{2}\frac{F_{ij}^2}{|\phi^\alpha|^2} + (D_i\phi^a)^2 + \frac{1}{\kappa^2}(1-\phi^3)^3(1+\phi^3). \tag{3.24}$$

To ensure that the solutions have finite energy we choose,

$$\lim_{\vec{x}\to 0}\phi^3 = -1, \quad \lim_{\vec{x}\to\infty}\phi^3 = 1. \tag{3.25}$$

Conditions on the fields A_i will be found for our radial field configuration.

3.3 Self-dual solutions

The inequality (3.23) is saturated when the inequalities (3.11) and (3.14) are saturated (for the sake of definiteness we have chosen the value of $\kappa = 1$, yielding the Bogomol'nyi equations,

$$F_{ij} = -\varepsilon_{ij}(1-\phi^3)^2(1+\phi^3) \tag{3.26}$$

$$\varepsilon_{ij}D_i\phi^a = \varepsilon^{abc}D_j\phi^b\phi^c, \tag{3.27}$$

where we have concentrated on the case of anti-self-duality. Our radially symmetric Ansatz for the fields A_i and $\vec{\phi}$ is again,

$$A_i = \frac{a(r)-N}{r}\varepsilon_{ij}\hat{x}_j \tag{3.28}$$

$$\phi^\alpha = \sin f(r)\, n^\alpha,\ \phi^3 = \cos f(r) \tag{3.29}$$

where $\vec{n} = (\cos N\theta, \sin N\theta)$ is a unit vector, with N an integer.

The Bogomol'nyi equations (3.26) and (3.27) now reduce to the following pair of coupled nonlinear first order ordinary differential equations,

$$\frac{a'}{r} = -(1-\cos f)^2(1+\cos f), \qquad f' = -\frac{a\sin f}{r}. \tag{3.30}$$

3.4 Non-self dual solutions

We will not study further the Bogomolny'i equations, as they have been investigated in detail in [14]. It should be noted that in the same publication, a proof of existence of the solitons has been given. In this model the $N = 1$ soliton was shown to exist, in contrast to the model studied in the previous chapter. In [11] a proof has been given of the nonexistence of the $N = 1$ soliton in the case of the $O(3)$ sigma model with a Maxwell term. We will now introduce a positive constant λ_0 in the potential (3.20). The case where λ_0 is equal to one has been discussed above. We will examine the Euler-Lagrange equations, now for positive λ_0 not necessarily equal to one.

Using the Ansatz (3.28),(3.29), with A_0 as in equation (3.8), the Hamiltonian reduces to the one dimensional subsystem,

$$\mathcal{L} = r\left[\left(\frac{a_r}{r\sin f}\right)^2 + f_r^2 + \left(\frac{a\,\sin f}{r}\right)^2 + \lambda_0(\sin^2 f(1-\cos f))^2\right], \tag{3.31}$$

defined by,

$$\int d^2x\, \mathcal{H}_0 = 2\pi \int dr\, \mathcal{L}. \tag{3.32}$$

When the one dimensional Lagrangian is varied the resulting equations are,

$$a(r)\sin^4 f + 2\cot f a_r f_r + \frac{a_r}{r} - a_{rr} = 0 \tag{3.33}$$

$$\lambda_0 r(1-\cos f)\sin f(\cos f - \cos^2 f + \sin^2 f) + \frac{a^2\cos f\sin f}{r} - \frac{\cot f\csc^2 f a_r^2}{r} - f_r - rf_{rr} = 0 \tag{3.34}$$

We first examine the equations (3.33) in the region $r \ll 1$ region. The solution is,

$$f(r) = \pi + f_o r^N + f_1 r^{N+2} + O(r^{N+4}) \tag{3.35}$$

$$a(r) = N + A_o r^{2N+2} + A_1 r^{2N+4} + O(r^{2N+4}), \tag{3.36}$$

where ,

$$N = 1 \begin{cases} f_1 = -\frac{24A_o^2+f_o^6-6f_o^4\lambda_0}{12f_o^3}, \\ A_1 = -\frac{8A_of_o^3-3f_o^5-48A_of_1}{36f_o}, \end{cases} \tag{3.37}$$

$$N \geq 2 \begin{cases} f_1 = -\frac{A_o^2(1+N)^2-f_o^4\lambda_0}{(1+N)f_o^3}, \\ A_1 = -\frac{2A_of_1(1+N)}{(2+N)f_o}. \end{cases} \tag{3.38}$$

The constants f_o and A_o are fixed by the asymptotic value of the solution at infinity. They are found by numerical methods, which require correct values of the fields at the boundary. Using a power series solution of the Bogomolny'i equations, it is found that the ratio

$$\frac{A_o}{f_o^2} = \frac{-1}{N+1} \tag{3.39}$$

holds. This gives one free parameter in the power series which controls the behaviour of the solutions. It will also serve as a check on the numerically evaluated constants.

Now considering the region $r \gg 1$ and anticipating decaying solutions, we linearise the Euler Lagrange equations about their asymptotic values. That is, the equations are linearised about $f = 0$ and around the asymptotic value $a(r) = \alpha$. The Euler Lagrange equation for $f(r)$ is linearised about its asymptotic value of zero, and found to be,

$$\alpha^2 F - rF_r - r^2 F_{rr} = 0.$$

The solutions to this are,

$$F = \frac{c_1}{r^\alpha} + c_2 r^\alpha.$$

In order to have finite energy solutions the constant c_2 is chosen as zero. The equation for $a(r)$ is also linearised, and found to be,

$$a_{rr} - ra_r = 0,$$

whose solution is $a = c_3 r^2$ or that a is a constant. The latter option is chosen, in order to restrict attention to finite energy solutions. This constant is chosen to be α. In the case of the analysis of the Bogomol'nyi equations there is found to be a restriction of the value of the constant α. It satisfies the inequality, $\alpha > \frac{1}{2}$.

3.5 Numerical analysis

We have studied the equations numerically using a shooting method. The integration started in the region $r \ll 1$ using as initial data the power series solutions. The constants f_o and A_o have been found which give the correct asymptotic behaviour. The profiles for the functions $f(r)$ for vorticity $n = 2, 4$ and those for $a(r)$ are given in figures 1,2,4,5, and the respective energy density profiles in figures 3 and 6.

In table 3 the total energies of the vortices have been calculated for the approximate solutions. If the Bogomolny'i equations are substituted into the one dimensional system the result is,

$$\mathcal{L} = -2f_r a \sin f - 2a_r(1 - \cos f) \tag{3.40}$$

The total energy of a topological self dual solution can be written as,

$$\begin{aligned} E_{sd} &= -2\int_0^\infty dr\,[a_r(1-\cos f) + a f_r \sin f]\,, && (3.41)\\ &= -2\int_0^\infty dr\,\frac{d}{dr}\left(a(1-\cos f)\right) && (3.42)\\ &= 4N. && (3.43) \end{aligned}$$

This last line is found using the boundary conditions for both functions $a(r)$ and $f(r)$.

The energy is independent of the choice of the number α. It is enough that $a_r \to 0$ as $r \to \infty$. The figures of the energy density for the value of constant $\lambda_0 = 1$ is the self-dual limit. It can be seen that the calculated values are close approximations to the analytic calculation. In figure 7, the values of total energy are plotted. For the $N = 2$ vortex, these figures are multiplied by 2. It can be seen that the $N = 4$ vortex energy is larger than the $N = 2$ energy, for the regime where $\lambda_0 < 1$. Also it can be seen that the $N = 2$ vortex energy is larger than the $N = 4$ energy, for the regime where $\lambda_0 > 1$. There is a, "cross over", between attraction and repulsion behaviour. The relations,

$$2\mathcal{E}(N = 2, \lambda_0 < 1) < \mathcal{E}(N = 4, \lambda_0 < 1), \tag{3.44}$$

$$2\mathcal{E}(N = 2, \lambda_0 > 1) > \mathcal{E}(N = 4, \lambda_0 > 1), \tag{3.45}$$

can be seen from the data, and in the graph. This states that a vortex with degree 2 is lighter that a vortex with degree 4, so it is energetically

favourable that vortices repel. Clearly in the second relation, attraction is favourable. The boundary conditions for the vortices were chosen to be the anti-self-dual configuration. When the vortices are self-dual, that is when $\lambda_0 = 1$ the energy of 4 vortices is twice that of 2 vortices. Only at the value of the constant $\lambda_0 = 1$ are the energies per unit vortex number equal. This means that there is no interaction enrergy between self-dual vortices. The values of the constants A_o and f_o for the self-dual solution should be related by equation (3.39). It is seen that the numerically calculated numbers are close to their theoretical ratio.

Figure 3.1: Profile of the function $f(r)$ for the vortices with $N = 2$ with $\lambda_0 = 1.2, \ldots, 0.8$ from left to right.

Figure 3.2: Profile of the function $a(r)$ for the vortices with $N = 2$ with lower values of α corresponding to lower λ_0.

Figure 3.3: Profile of the energy density for the $N = 2$ vortices where increasing peaks represent increasing energy and increasing λ_0.

Figure 3.4: Profile of the function $f(r)$ for the vortices with $N = 4$ with $\lambda_0 = 1.2, \ldots, 0.8$ from left to right.

Figure 3.5: Profile of the function $a(r)$ for the vortices with $N = 4$ with lower values of α corresponding to lower λ_0.

Figure 3.6: Profile of the energy density for the $N = 4$ vortices where increasing peaks represent increasing energy and increasing λ_0.

Figure 3.7: Graph of the energy of two superimposed vortices, $2\mathcal{E}(\lambda_0, N = 2)$ and $\mathcal{E}(\lambda_0, N = 4)$, as a function of λ_0.

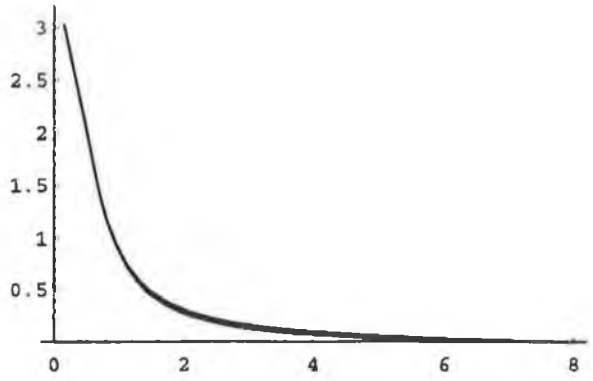

Figure 1

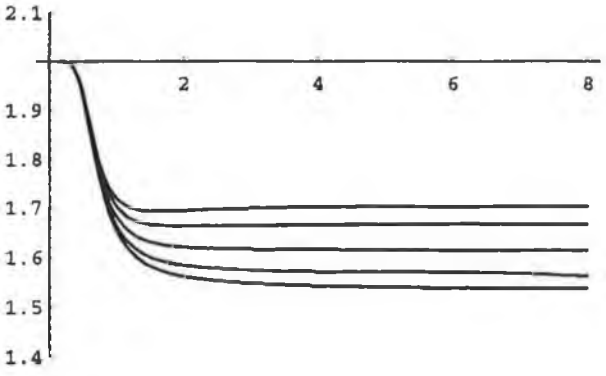

Figure 2

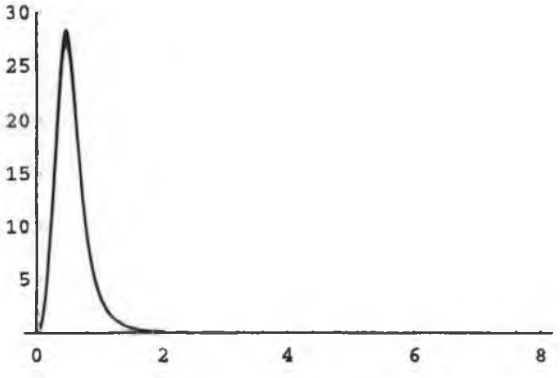

Figure 3

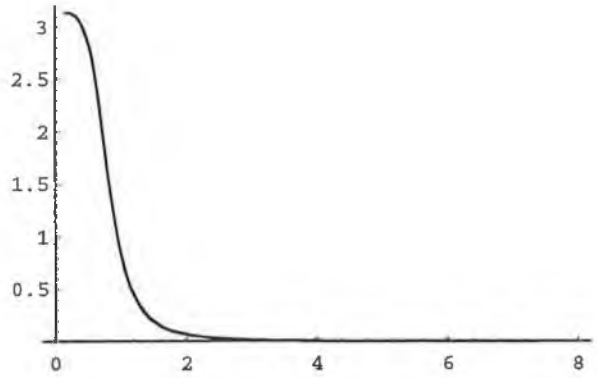

Figure 4

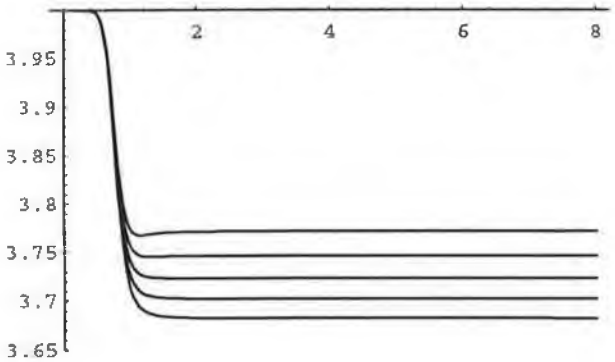

Figure 5

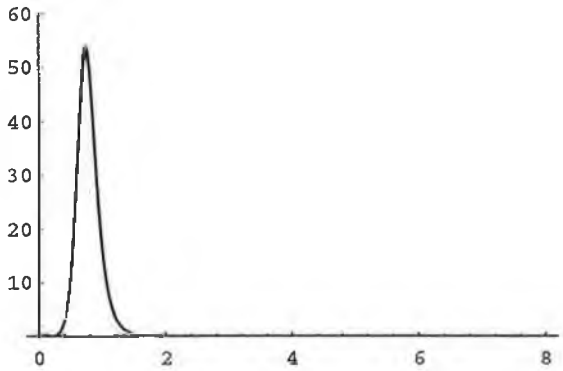

Figure 6

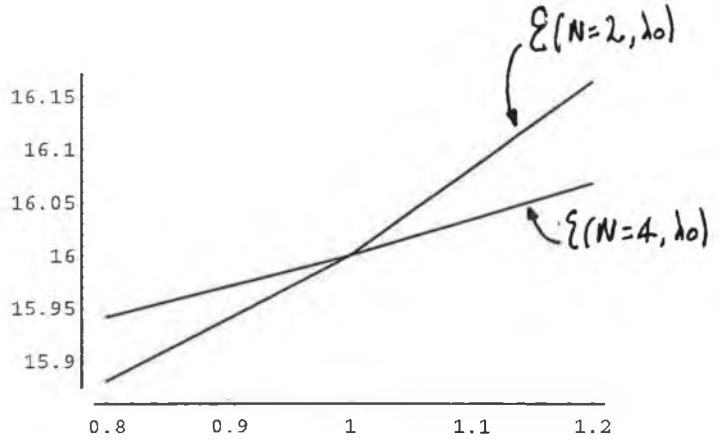
$\mathcal{E}(N=2,\lambda_0)$
$\mathcal{E}(N=4,\lambda_0)$
16.15
16.1
16.05
16
15.95
15.9
0.8
0.9
1
1.1
1.2

Figure 7

Constants	$N = 2$	
λ	A_o	f_o
0.8	-7.90372	-5.0000
0.9	-8.09182	-5.0000
1.0	-8.33333	-5.0000
1.1	-8.53843	-5.0000
1.2	-8.65862	-5.0000

Table 3.1: Numerically calculated values of the constants in the power series (3.36) for $N = 2$.

Constants	$N = 4$	
λ	A_o	f_o
0.8	-4.68536	-5.00000
0.9	-4.85028	-5.00000
1.0	-5.00000	-5.00000
1.1	-5.13790	-5.00000
1.2	-5.26629	-5.00000

Table 3.2: Numerically calculated values of the constants in the power series (3.36) for $N = 4$.

Constants	Energy	
λ	$E(\lambda_0, N = 2)$	$E(\lambda_0, N = 4)$
0.8	7.9408	15.9423
0.9	7.9694	15.9695
1.0	8.0000	16.0000
1.1	8.0411	16.0330
1.2	8.0819	16.0680

Table 3.3: Numerically calculated values of the energy in units of 2π for vorticity $N = 2, 4$.

Chapter 4

The Abelian Chern-Simons-Higgs model.

4.1 Introduction

The purpose of this chapter is to present a further model and in particular, a computation of the interaction energy of Chern-Simons vortices which are infinitely separated. The results will show the behaviour of the interaction energy as a function of the coupling constant, which measures the relative strength of the matter self-coupling and the electromagnetic coupling. In our normalisation convention, the region $\lambda_0 < \frac{1}{2}$, the strength of matter self interaction exceeds that of the electromagnetic interaction. In the region $\lambda_0 > \frac{1}{2}$ the opposite is true. We find that vortices attract each other for $\lambda_0 < \frac{1}{2}$ and repel when $\lambda_0 > \frac{1}{2}$. When $\lambda_0 = \frac{1}{2}$ there is a lower bound on the energy that can be saturated. In the case that the bound is saturated, then the fields satisfy a set of first order partial differential equations. These results are analogous to the results of Jacobs and Rebbi [12], who analysed the Abelian Higgs model. The results in this chapter have appeared in [13].

The study of vortices which has been extensively used in the study of particle physics now finds uses in the study of condensed matter physics. The physics of the recently discovered high-T_c superconductors is an important problem. Studies of Chern-Simons (C-S) solitons can be related to the unusual behaviour of this new type of superconductor. Self-dual Chern-Simons vortices were first introduced by Hong *et. al.* [16] and Jackiw *et. al.* [17].

Here we consider certain new aspects of the model.

4.2 The model

We shall, again, label (2+1) space coordinates by Greek indices $\mu, \nu, \ldots$, and in the static case the coordinates of R^2 by Latin indices. Our model in $2+1$ dimensions is,

$$\mathcal{L} = D^\mu \phi \overline{D_\mu \phi} + \frac{\kappa}{4} \epsilon^{\alpha\beta\gamma} A_\alpha F_{\beta\gamma} - V(|\phi|) \tag{4.1}$$

where the $U(1)$ covariant derivative is $D_\mu = \partial_\mu + iA_\mu$ having curvature $F_{\mu\nu} = \partial_\mu A_\nu - \partial_\nu A_\mu$. The field ϕ is a complex function. and the self interation potential will be chosen later to be $V(|\phi|) = \frac{\lambda_0}{4}|\phi|^2(1-|\phi|^2)^2$, due to requirements of topological stability. The constant κ has the dimensions of a length.

Variation of the action leads to the equations,

$$D_\mu D^\mu \phi + \frac{\partial V}{\partial \phi^*} = 0 \tag{4.2}$$

$$\frac{1}{2}\kappa \epsilon^{\alpha\beta\gamma} F_{\beta\gamma} - J^\alpha = 0 \tag{4.3}$$

where the conserved matter current is given by

$$J^\alpha = i(\phi^* D^\alpha \phi - \phi \overline{D^\alpha \phi}). \tag{4.4}$$

The time component of equation (4.3) in the static limit is,

$$\frac{\kappa}{2} \varepsilon^{ij} F_{ij} = -2A^0 |\phi|^2 \tag{4.5}$$

This is the Chern-Simons version of Gauss' law, and can be used to solve for A^0 in the static limit giving,

$$A^0 = -\frac{\kappa}{4} \frac{\varepsilon^{ij} F_{ij}}{|\phi|^2}. \tag{4.6}$$

For definiteness we now choose $\kappa = 2\sqrt{2}$.

The energy momentum tensor is found by varying the Lagrangian (4.1) with respect to the metric,

$$T_{\mu\nu} = \overline{D_\mu \phi} D_\nu \phi + D_\mu \phi \overline{D_\nu \phi} - g_{\mu\nu}(D^\rho \phi \overline{D_\rho \phi} - V). \tag{4.7}$$

The Hamiltonian density is,

$$\mathcal{H} = \overline{D_0\phi} D_0\phi + D_i\phi\overline{D_i\phi} + V. \tag{4.8}$$

where $\mathcal{H}_0$, the corresponding static potential energy density is,

$$\begin{aligned} \mathcal{H}_0 &= (-iA_0\phi^*)(iA_0\phi) + D_i\phi\overline{D_i\phi} + V & (4.9)\\ &= \frac{F_{ij}^2}{|\phi|^2} + D_i\phi\overline{D_i\phi} + V. & (4.10) \end{aligned}$$

Here the Chern-Simons Gauss' law, (4.6), has been used to obtain the second equality.

Occurrence or absence of topologically stable vortex solutions of the model can be inferred from the inequalities,

$$|(D_i\phi - i\epsilon_{ij}D_j\phi)|^2 \geq 0 \tag{4.11}$$

$$(\frac{1}{|\phi|}F_{ij} - \sqrt{\frac{\lambda_0}{4}}\frac{\epsilon_{ij}}{\sqrt{2}}|\phi|(1-|\phi|^2))^2 \geq 0. \tag{4.12}$$

These can be rewritten as,

$$\frac{F_{ij}^2}{|\phi|^2} + \frac{\lambda_0}{4}|\phi|^2(1-|\phi|^2)^2 \geq \epsilon_{ij}F_{ij}\sqrt{\frac{\lambda_0}{2}}(1-|\phi|^2) \tag{4.13}$$

$$|D_i\phi|^2 \geq -i\epsilon_{ij}\partial_i(\phi\overline{D_j\phi}) + \frac{1}{2}\epsilon_{ij}F_{ij}|\phi|^2. \tag{4.14}$$

The inequalities (4.13,4.14) lead to an energy that is bounded below by a surface integral if $\lambda_0 = \frac{1}{2}$. In this case,

$$\begin{aligned} \mathcal{H}_0 &= \frac{F_{ij}^2}{|\phi|^2} + D_i\phi\overline{D_i\phi} + \frac{1}{8}|\phi|^2(1-|\phi|^2)^2 & (4.15)\\ &\geq \epsilon_{ij}\partial_i(A_j - i\phi\overline{D_j\phi}) & (4.16)\\ &\equiv \partial_i\Omega_i. & (4.17) \end{aligned}$$

We see that $V(|\phi|)$ in (4.1) is now determined by the requirement that the surface integral is bounded below by a total divergence,

$$V = \frac{1}{8}|\phi|^2(1-|\phi|^2)^2.$$

4.3 Self-dual solutions

The self-dual equations may be found by saturating the inequalities (4.13) and (4.14), giving the Bogomol'nyi equations [17],

$$D_i\phi = i\epsilon_{ij}D_j\phi \tag{4.18}$$

$$\frac{1}{|\phi|}F_{12} = \frac{1}{4}|\phi|(1-|\phi|^2). \tag{4.19}$$

Finite-energy field configurations are divided into classes containing those field configurations which can be continuously deformed into each other. The solutions we shall present are radially symmetric fields of vorticity n given by,

$$\begin{aligned} \phi(r,\theta) &= f(r)\exp(in\theta) \\ A_i &= -\epsilon_{ij}\frac{nx_j}{r^2}a(r), \end{aligned} \tag{4.20}$$

where, as before, $r^2 = x_ix_i$ and θ is the azimuthal angle. In order that the fields be nonsingular at the origin, we impose the boundary conditions at the origin,

$$f(0) = a(0) = 0.$$

At spatial infinity, to satisfy the requirement of finite energy, we demand,

$$\lim_{r\to\infty} f(r) = 1, \quad \lim_{r\to\infty} a(r) = 1. \tag{4.21}$$

The Bogomol'nyi equations for this Ansatz lead to,

$$f_r = \frac{nf}{r}(1-a) \tag{4.22}$$

$$\frac{na_r}{r} = -\frac{1}{4}f^2(f^2-1), \tag{4.23}$$

The self dual solutions will not be further discussed, but we shall proceed directly to the solutions of the Euler-Lagrange equations, for λ_0 not necessarily equal to $\frac{1}{2}$.

4.4 Non-self-dual solutions

Using the ansatz, (4.20), the static Hamiltonian reduces to the one dimensional subsystem:

$$\mathcal{L} = \frac{1}{r}(nf(1-a))^2 + r(f_r)^2 + \frac{2r}{f^2}\left(\frac{na_r}{r}\right)^2 + r\frac{\lambda_0}{4}f^2(f^2-1)^2, \tag{4.24}$$

defined by,

$$\int d^2x\mathcal{H}_0 = 2\pi\int dr\mathcal{L}. \tag{4.25}$$

Subjecting the one dimensional subsystem (4.25) to the variational principle, we obtain the following Euler-Lagrange equations,

$$\frac{2n^2}{r}(1-a)^2 f + \frac{\lambda_0 r}{2}f(1-f^2)(1-3f^2) - \frac{4n^2a_r^2}{rf^3} - 2f_r - 2rf_{rr} = 0 \tag{4.26}$$

$$-\frac{2n^2}{r}(1-a)f^2 + \frac{4n^2a_r^2}{r^2f^2} + \frac{8n^2a_rf_r}{rf^3} - \frac{4n^2a_{rr}}{rf^2} = 0. \tag{4.27}$$

Solutions of these equations lead to solutions of the full Euler-Lagrange equations. We first examine equations (4.26) and (4.27) in the $r \gg 1$ region, and anticipating exponentially decaying solutions, we linearise them in the functions $F(r)$ around the asymptotic value $f = 1$, and $A(r)$ around the asymptotic value $a = 1$. The linearised second order equations are,

$$r^2F_{rr} + rF_r - \lambda_0 r^2F = 0 \tag{4.28}$$

$$r^2A_{rr} - rA_r - \frac{1}{2}r^2A = 0 \tag{4.29}$$

independent of vorticity n. The solutions of equations (4.28) and (4.29) are, respectively, the modified Bessel functions

$$F(r) = K_0(\sqrt{\lambda_0}r) \tag{4.30}$$

$$A(r) = rK_1(\frac{1}{\sqrt{2}}r). \tag{4.31}$$

From this we see that the topological solitons for this system decay exponentially.

Next we examine the asymptotic solutions of equations (4.26) and (4.27) in the range $r \ll 1$. We attempt power series solutions and obtain,

$$f(r) = f_n r^n + f_{n+2} r^{n+2} + O(r^{n+4}) \tag{4.32}$$
$$a(r) = a_{2n+2} r^{2n+2} + a_{2n+4} r^{2n+4} + O(r^{2n+6}) \tag{4.33}$$

$$f_{n+2} = \frac{\lambda_0 f_n^4 - 32n^2 a_{2n+2}^2 (1+n)^2}{16 f_n (1+n)} \tag{4.34}$$
$$a_{2n+4} = \frac{-f_n^5 + 32 a_{2n+2} f_{n+2}}{24 f_n} \quad , n = 1 \tag{4.35}$$
$$a_{2n+4} = \frac{2 a_{2n+2} f_{n+2} (1+n)}{f_n (2+n)} \quad , n \geq 2 \tag{4.36}$$

where f_n and a_{2n+2} are arbitrary constants to be fixed by the numerical integrations in the next section. When a power series solution for the Bogomol'nyi equations of the form (4.33) is attempted for these equations, the ratio,

$$\frac{a_{2n+2}}{f_n^2} = \frac{1}{4n(2n+2)} \tag{4.37}$$

holds. This will be a check on the numerical values of the constants evaluated for the self-dual equations.

If the Bogomol'nyi equations are substituted into the one dimensional system, the result is,

$$\mathcal{L}_{sd} = 2n(1-a) f f_r - n a_r (f^2 - 1). \tag{4.38}$$

The total energy of a self dual solution can be written as,

$$\mathcal{E}_{sd} = \int_0^\infty dr \mathcal{L}_{sd} = \int_0^\infty \frac{d}{dr} \Big(n(1-a)(f^2-1) \Big) \, dr \tag{4.39}$$
$$= n. \tag{4.40}$$

This is found by using the boundary conditions for both the functions $a(r)$ and $f(r)$. The figures for the total energy for the value of the constant $\lambda_0 = \frac{1}{2}$ is the self dual limit.

4.5 Numerical analysis

We have studied equations (4.26) and (4.27) numerically using a shooting method and have found solutions with the correct asymptotic behaviour (4.30) and (4.31). The integration is started in the region $r \ll 1$ using the appropriate data given by (4.32) and (4.33). We have found those values of the constants f_n and a_{2n+2} for which the functions f and a tend to the asymptotic value given by (4.21) corresponding to the behaviour given by (4.32) and (4.33) in the $r \gg 1$ region.

The profiles for the functions $f(r)$ for vorticity $n = 1, 2$ and $a(r)$ for vorticity $n = 1, 2$ are given in figures $1, 2, 3, 4$ respectively. There are six profiles in each graph, with $\lambda_0 = 0.8, 0.7, \ldots, 0.2$ going from left to right. The corresponding graphs for energy are given in figures 5 and 6 for $n = 1, 2$ respectively, where increasing peaks represent increasing energy, and increasing λ_0. The energy for the $n = 1$ vortices are concentrated in balls, while that of the $n = 2$ vortices is concentrated in rings. The values of the energy and the corresponding value of λ_0 for each of the vorticities are given in table 3. The energy of the $n = 2$ vortex is larger than twice the energy of the $n = 1$ vortex for $\lambda_0 > \frac{1}{2}$. This means that the forces between two solitons of unit vorticity are repulsive. The energy of the $n = 2$ vortex is less than twice the energy of the $n = 1$ vortex for $\lambda_0 < \frac{1}{2}$. In this case the forces between two solitons of unit vorticity are attractive. In the self dual limit, $\lambda_0 = \frac{1}{2}$, the energies of the $n = 2$ vortex equals twice the energy of the $n = 1$ vortex, to within 1 part in 10^6. In figure 7 the twice the energy of the $n = 1$ vortex and the energy of the $n = 2$ vortex is plotted on the same axes as a function of λ_0. In the Bogomol'nyi limit the diagonal components of the stress tensor vanish; $T_{11} = T_{22} = 0$. This means that there is no interaction of the vortices. We have examined the ratio (4.37) in the Bogomol'nyi limit for the values of the constants a_{2n+2} and f_n, found by integrating the Euler-Lagrange equations (4.26,4.27), for $n = 1, 2$. We find that the numerical values agree with the exact values to seven decimal places. In the case $n = 1$ the value of the ratio (4.37) is $\frac{1}{16} = 0.0625$, for the numerical values in table 1, the ratio is 0.0625. In the $n = 2$ case the value of the ratio (4.37) is $\frac{1}{48} = 0.02083$, for the numerical values in table 2, the ratio is 0.02083.

We will comment briefly on the results. The evaluation of the profile functions can contain numerical errors inherent in the approximation of the solutions of differential equations. An estimate of the accuracy is provided

by considering the values of

$$\begin{aligned} \mathcal{E}(n=1,\lambda_0=\frac{1}{2}) &= 0.99999 \\ \mathcal{E}(n=2,\lambda_0=\frac{1}{2}) &= 1.99999 \end{aligned}$$

calculated numerically and those $\mathcal{E}(n=1,\lambda_0=\frac{1}{2})=1$ and $\mathcal{E}(n=2,\lambda_0=\frac{1}{2})=2$ calculated analytically. The results for $\lambda_0=0.3$ and $\lambda_0=0.8$ show clearly how vortices attract and repel each other respectively.

We have considered a Lagrangian with Chern Simons term and a sextic potential for which we have shown that self dual solutions exist. We have shown rigorously that they had topological stability by showing that they have a Bogomol'nyi limit and find "crossover", that is attraction and repulsion.

Figure 4.1: Profile of the function $f(r)$ for the vortices with $n = 1$ with $\lambda_0 = 0.8, \ldots, 0.3$ from left to right.

Figure 4.2: Profile of the function $f(r)$ for the vortices with $n = 2$ with $\lambda_0 = 0.8, \ldots, 0.3$ from left to right.

Figure 4.3: Profile of the function $a(r)$ for the vortices with $n = 1$ with $\lambda_0 = 0.8, \ldots, 0.3$ from left to right.

Figure 4.4: Profile of the function $a(r)$ for the vortices with $n = 2$ with $\lambda_0 = 0.8, \ldots, 0.3$ from left to right.

Figure 4.5: Profile of the energy density for the $n = 1$ vortices where increasing peaks represent increasing energy and increasing λ_0.

Figure 4.6: Profile of the energy density for the $n = 2$ vortices where increasing peaks represent increasing energy and increasing λ_0.

Figure 4.7: Graph of the energy of two superimposed vortices, $\mathcal{E}(\lambda_0, n = 2)$ and twice the energy of a single vortex, $2\mathcal{E}(\lambda_0, n = 1)$ as a function of λ_0.

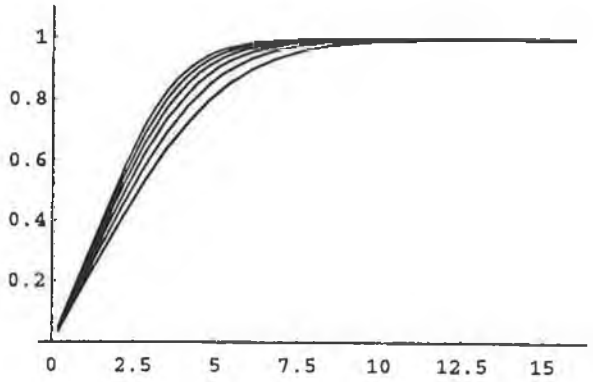

Figure 1

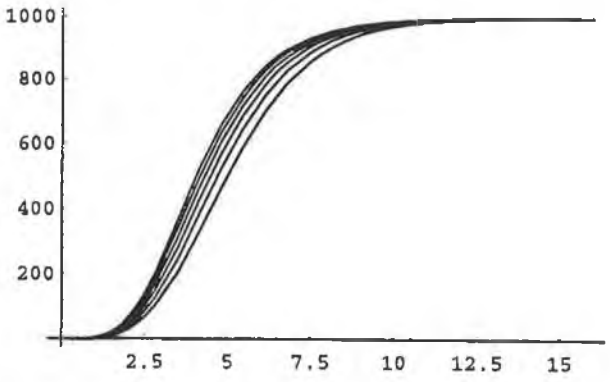

Figure 3

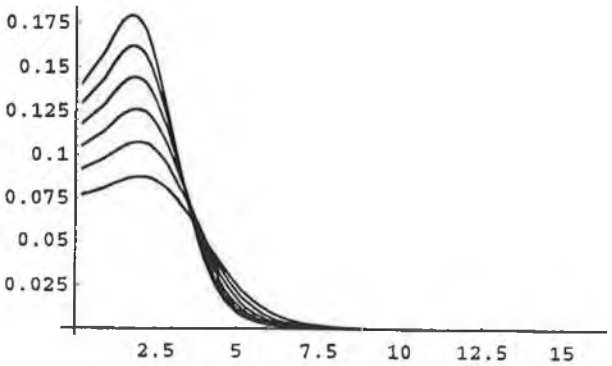

Figure 5

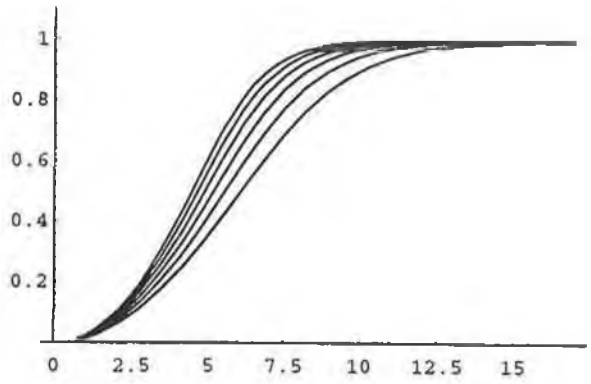

Figure 2

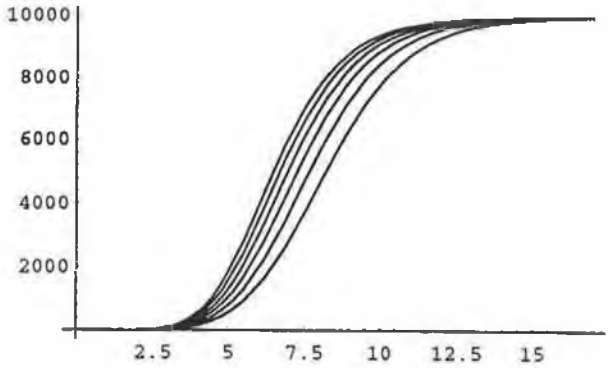

Figure 4

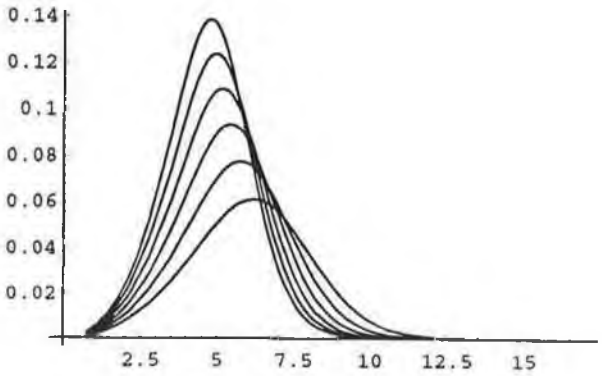

Figure 6

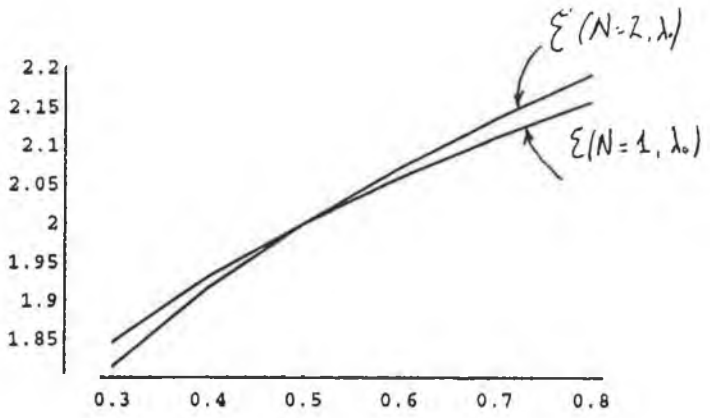
$\mathcal{E}(N=2,\lambda_0)$
$\mathcal{E}(N=1,\lambda_0)$
2.2
2.15
2.1
2.05
2
1.95
1.9
1.85
0.3
0.4
0.5
0.6
0.7
0.8

Figure 7

Constants	$n = 1$	
λ_0	$10^3 a_{2n+2}$	f_n
0.3	2.16141	0.19628
0.4	2.73060	0.21403
0.5	3.27769	0.22900
0.6	3.80833	0.24207
0.7	4.32600	0.25376
0.8	4.83310	0.26438

Table 4.1: Table of the constants a_{2n+2} and f_n found using the shooting method for $n = 1$.

Constants	$n = 2$	
λ_0	$10^4 a_{2n+2}$	f_n
0.3	0.04198	0.01506
0.4	0.05999	0.01741
0.5	0.07910	0.01948
0.6	0.09906	0.02134
0.7	0.11973	0.02304
0.8	0.14099	0.02461

Table 4.2: Table of the constants a_{2n+2} and f_n found using the shooting method for $n = 2$.

Constants	Energy	
λ_0	$\mathcal{E}(n = 1, \lambda_0)$	$\mathcal{E}(n = 2, \lambda_0)$
0.3	0.92301	1.81468
0.4	0.96536	1.91629
0.5	0.99999	1.99999
0.6	1.02951	2.07174
0.7	1.05535	2.13487
0.8	1.07841	2.19144

Table 4.3: Table of the numerically calculated energies for both $n = 1$ and $n = 2$.

Chapter 5

Zero modes of Abelian Yang-Mills-Higgs vortices

5.1 Introduction

In this chapter we present yet another model. We calculate its radially symmetric self-dual solutions. We will examine the static vortices of the Abelian Yang-Mills-Higgs model. The attraction and repulsion behaviour of the vortices in this model is well known, [12], so we will not repeat the analysis. We will calculate the zero modes around the radially symmetric solutions [18]. The asymptotic properties of the solutions will be examined. These solutions will be used in the next chapter to provide initial data for the Cauchy problem.

5.2 The Abelian Higgs model

We shall label $(2+1)$ space coordinates by Greek indices $\mu, \nu, \ldots$, and in the static case the coordinates of R^2 by Latin indices. Our model in $2+1$ dimensions is,

$$\mathcal{L} = \frac{1}{2} D^{\mu}\Phi \overline{D_{\mu}\Phi} - \frac{1}{4} F^{\mu\nu} F_{\mu\nu} - V(|\Phi|) \tag{5.1}$$

where the $U(1)$ covariant derivative is $D_{\mu} = \partial_{\mu} - iA_{\mu}$ having curvature $F_{\mu\nu} = \partial_{\mu} A_{\nu} - \partial_{\nu} A_{\mu}$, and the self interation potential $V(|\Phi|) = \frac{\lambda}{8}(|\Phi|^2 - 1)^2$. The indices are raised and lowered with the metric tensor $g = \mathrm{diag}(+1, -1, -1)$.

The field Φ is a complex valued field, and is a scalar function in contrast the the matter fields of the sigma models. It is sometimes called the "Higgs field". Variation of the action leads to the Euler-Lagrange equations,

$$D_\mu D^\mu \Phi + \frac{\lambda}{2}\Phi(|\Phi|^2 - 1) = 0, \tag{5.2}$$

$$\partial_\mu F^{\mu\nu} + \frac{i}{2}(\Phi^*(D^\nu\Phi) - \Phi(\overline{D^\nu\Phi})) = 0. \tag{5.3}$$

For all λ the Euler-Lagrange equations have static, finite energy n-vortex solutions of the form [20],

$$A_i(r,\theta) = -\epsilon_{ij}x^j n\frac{a(r)}{r^2},\ A_0 = 0,\quad \Phi(r,\theta) = f(r)\exp[in\theta], \tag{5.4}$$

for $i,j = 1,2$, where,

$$r\frac{d}{dr}\left(\frac{1}{r}\frac{da}{dr}\right) - f^2(r)[a(r) - 1] = 0, \tag{5.5}$$

$$2r\frac{d}{dr}\left(r\frac{df}{dr}\right) - 2n^2 f(r)[a(r) - 1]^2 - \lambda r^2 f(r)[f^2(r) - 1] = 0. \tag{5.6}$$

In order that the fields be nonsingular at the origin we impose the boundary conditions at the origin,

$$f(0) = 0,\quad a(0) = 0. \tag{5.7}$$

At spatial infinity, the requirement of finite energy demands,

$$\lim_{r\to\infty} f(r) = \lim_{r\to\infty} a(r) = 1. \tag{5.8}$$

The energy momentum tensor is found by varying the Lagrangian (5.1) with respect to the metric,

$$T_{\mu\nu} = \frac{1}{2}(\overline{D_\mu\Phi}D_\nu\Phi + D_\mu\Phi\overline{D_\nu\Phi}) - F_{\mu\rho}F^\rho_\nu - g_{\mu\nu}(\frac{1}{2}D_\rho\Phi\overline{D^\rho\Phi} - \frac{1}{4}F_{\rho\lambda}F^{\rho\lambda} - V). \tag{5.9}$$

The static Hamiltonian density $\mathcal{H}_0$ is,

$$\mathcal{H}_0 = \frac{1}{2}\overline{D_i\Phi}D_i\Phi + \frac{1}{4}F_{ij}F_{ij} + V. \tag{5.10}$$

Occurrence or absence of topologically stable vortex solutions of the model can be inferred from the following inequalities,

$$|(D_i\Phi + i\epsilon_{ij}D_j\Phi)|^2 \geq 0 \tag{5.11}$$

$$(\frac{1}{2}F_{ij} - \sqrt{\frac{\lambda}{8}}\frac{\epsilon_{ij}}{\sqrt{2}}(1-|\Phi|^2))^2 \geq 0 \tag{5.12}$$

which can be rewritten as,

$$\frac{1}{4}F_{ij}^2 + \frac{\lambda}{8}(1-|\Phi|^2)^2 \geq \sqrt{\frac{\lambda_0}{16}}\epsilon_{ij}F_{ij}(1-|\Phi|^2) \tag{5.13}$$

$$|D_i\Phi|^2 \geq i\epsilon_{ij}\partial_i(\Phi\overline{D_j\Phi}) + \frac{1}{2}\epsilon_{ij}F_{ij}|\Phi|^2. \tag{5.14}$$

The inequalities (5.13,5.14) lead to an energy that is bounded below by a surface integral if $\lambda = 1$ and, in that case it follows that,

$$\mathcal{H}_0 = \frac{1}{4}F_{ij}^2 + \frac{1}{2}D_i\Phi\overline{D_i\Phi} + \frac{1}{8}(1-|\Phi|^2)^2 \tag{5.15}$$

$$\geq \frac{1}{2}\epsilon_{ij}\partial_i(A_j - i\Phi D_j\Phi^*) \tag{5.16}$$

$$\equiv \partial_i\Omega_i. \tag{5.17}$$

To ensure finite energy configurations we require,

$$\lim_{r\to\infty}|\Phi|^2 = 1. \tag{5.18}$$

The field Φ becomes a unimodular number as $r \to \infty$. Together with the condition that the covariant derivative vanishes, this is essential for the proof that the integral (5.17) is equal to the winding number, n. We have,

$$n = \frac{1}{2\pi}\int \epsilon^{ij}\partial_i A_j \, d^2x. \tag{5.19}$$

The self-dual equations may be found by saturating the inequalities (4.13) and (4.14), giving the Bogomol'nyi equations;

$$(D_1 + iD_2)\Phi = 0 \tag{5.20}$$

$$F_{12} = -\frac{1}{2}(|\Phi|^2 - 1). \tag{5.21}$$

5.3 Fluctuation equations and zero modes

We consider solutions to the Bogomol'nyi equations in the form of a series in α,

$$\Phi = \hat{\phi} + \alpha\zeta + \alpha^2\eta \tag{5.22}$$
$$A_i = \hat{A}_i + \alpha a_i + \alpha^2\beta_i. \tag{5.23}$$

The equations at orders of the parameter α which follow from equation (5.20) are,

$$\alpha^0, \quad \hat{D}_1 + i\hat{D}_2)\hat{\phi} = 0, \tag{5.24}$$
$$\alpha^1, \quad (\hat{D}_1 + i\hat{D}_2)\zeta - i(a_1 + ia_2)\hat{\phi}) = 0, \tag{5.25}$$
$$\alpha^2, \quad (\hat{D}_1 + i\hat{D}_2)\eta - i(\beta_1 + i\beta_2)\hat{\phi} - i(a_1 + ia_2)\zeta = 0, \tag{5.26}$$

where $\hat{D}_i = \partial_i - i\hat{A}_i$. An expansion for equation (5.21) is also found,

$$\alpha^0, \quad \hat{F}_{12} = \frac{1}{2}(|\hat{\phi}|^2 - 1), \tag{5.27}$$
$$\alpha^1, \quad (\partial_1 a_2 - \partial_2 a_1) = -\frac{1}{2}(\hat{\phi}\zeta^* + \hat{\phi}^*\zeta), \tag{5.28}$$
$$\alpha^2, \quad (\partial_1\beta_2 - \partial_2\beta_1) = -\frac{1}{2}(\hat{\phi}\eta^* + \hat{\phi}^*\eta + \zeta\zeta^*). \tag{5.29}$$

It has been shown that a solution to the static Euler-Lagrange equations exists. It describes $n-$vortices superimposed at the origin,

$$\hat{A}_i(r,\theta) = \epsilon_{ij}x^j\frac{na(r)}{r^2},$$
$$\hat{A}_0 = 0,$$
$$\hat{\phi} = f(r)\exp(in\theta).$$

This solution is substituted into equations (5.24) and (5.27), and it is seen that the functions $a(r)$ and $f(r)$ satisfy,

$$r\frac{df}{dr} - n(1 - a(r))f(r) = 0, \tag{5.30}$$
$$\frac{2n}{r}\frac{da(r)}{dr} + f(r)^2 - 1 = 0. \tag{5.31}$$

These are the static finite energy solutions about which we expand the fields and calculate the fluctuations.

We write fluctuations about the rotationally symmetric solutions in the form,

$$\delta\phi = \zeta = ne^{in\theta} f(r)h(r,\theta) \tag{5.32}$$

$$\begin{pmatrix} \delta A_1 \\ \delta A_2 \end{pmatrix} = \begin{pmatrix} a_1 \\ a_2 \end{pmatrix} = \frac{n}{r} \begin{pmatrix} -\sin\theta & \cos\theta \\ \cos\theta & \sin\theta \end{pmatrix} \begin{pmatrix} b(r,\theta) \\ c(r,\theta) \end{pmatrix} \tag{5.33}$$

The function $h(r,\theta)$ can be written as the sum of its real and imaginary parts as $h_1(r,\theta) + ih_2(r,\theta)$. Note that if we have a solution to the linearised equations, any multiple of it is also a solution. In particular, if we take t times the solution, it is still a solution to the linearized Bogomol'nyi equations. Solutions of the Bogomol'nyi equations satisfy the full time dependent linearised Euler-Lagrange equations. A function comprising of a static solution added to t times a solution of the linearised Bogomoln'yi equations is a solution of the full time dependent Euler-Lagrange equations linearised about the fluctuations.

When the ansatz for the fluctuations is substituted into equation (5.25) the real part of the equation is,

$$\frac{\partial h_1}{\partial r} - \frac{1}{r}\frac{\partial h_2}{\partial \theta} + \frac{b}{r} = 0. \tag{5.34}$$

The imaginary part of the equation is,

$$\frac{1}{r}\frac{\partial h_1}{\partial \theta} + \frac{\partial h_2}{\partial r} - \frac{1}{r}c = 0. \tag{5.35}$$

When the ansatz is substituted into equation (5.28) the result is,

$$\frac{1}{r}\frac{\partial b}{\partial r} - \frac{1}{r^2}\frac{\partial c}{\partial \theta} + f^2 h_1 = 0. \tag{5.36}$$

Using the equations (5.34,5.35,5.36) a single equation for $h_1(r,\theta)$ is found, namely,

$$\frac{1}{r}\frac{\partial}{\partial r}\left(r\frac{\partial h_1}{\partial r}\right) + \frac{1}{r^2}\frac{\partial^2 h_1}{\partial \theta^2} - f^2 h_1 = 0. \tag{5.37}$$

The equation of motion associated with A_0, which is the Gauss law must be imposed as a constraint,

$$-\partial_i \partial_t A_i + \frac{i}{2}(\Phi^* \partial_t \Phi - \Phi \partial_t \Phi^*) = 0. \tag{5.38}$$

We are considering fluctuations in the neighbourhood of the rotationally symmetric vortices. This allows us to say that the function $\alpha = \alpha(t)$ is linear in time, for $t \ll 1$. In order to find an equation for $h_2(r, \theta)$ the ansatz for the fluctuation is substituted into (5.38),

$$\partial_i a_i + \frac{i}{2}(\phi^* \zeta - \phi \zeta^*) = 0. \tag{5.39}$$

This yields,

$$\frac{1}{r}\frac{\partial c}{\partial r} + \frac{1}{r^2}\frac{\partial b}{\partial \theta} - f^2 h_2 = 0. \tag{5.40}$$

The equations (5.34,5.35) can be combined with (5.40) to give an equation for $h_2(r, \theta)$, namely,

$$\frac{1}{r}\frac{\partial}{\partial r}\left(r\frac{\partial h_2}{\partial r}\right) + \frac{1}{r^2}\frac{\partial^2 h_2}{\partial \theta^2} - f^2 h_2 = 0, \tag{5.41}$$

which is identical to (5.37). If the relation $h(r, \theta) = h_1(r, \theta) + i h_2(r, \theta)$ is used, the two equations can be combined into one,

$$r h_{rr} + h_r + \frac{1}{r} h_{\theta\theta} - r f^2 h = 0. \tag{5.42}$$

In order to obtain solutions to this partial differential equation, the function $h(r, \theta)$ is expanded as,

$$h(r, \theta) = \sum_{k=0}^{\infty} \left(h_k^{(1)}(r) \cos k\theta + h_k^{(2)}(r) \sin k\theta \right), \tag{5.43}$$

and substituted into equation (5.42). The equation satisfied by $h_k^{(i)}$ is

$$\frac{1}{r}\frac{d}{dr}\left(r\frac{dh_k^{(i)}}{dr}\right) - \left(f^2 + \frac{k^2}{r^2}\right) h_k^{(i)} = 0. \tag{5.44}$$

5.4 Asymptotic properties of the solutions

The differential equations that the functions $a(r), f(r)$ and $h(r)$ satisfy are the Euler-Lagrange equations respectively,

$$\frac{d}{dr}\left(\frac{a'(r)}{r}\right) - \frac{f^2(a-1)}{r} = 0 \tag{5.45}$$

$$(rf')' - \frac{n^2 f}{r}(a-1)^2 - \frac{\lambda}{2} r f(f^2-1) = 0 \tag{5.46}$$

$$r^2 h'' + rh' - h(k^2 + r^2 f^2) = 0. \tag{5.47}$$

Series solutions of the following form are attempted for the equations,

$$a(r) = \sum_{j=2}^{\infty} a_j r^j, \quad f(r) = \sum_{j=n}^{\infty} f_j r^j, \quad h(r) = \sum_{j=-k}^{\infty} h_j r^j.$$

The coefficients satisfy certain relations. For $q \leq 2n+3$, a_q is found from

$$\sum_{j=2}^{2n+3} j(j-2) a_j r^j - \sum_{m=2n+2}^{2n+3} \sum_{j=n}^{m-3} f_j f_{m-j-2} r^m = 0.$$

From which it is seen that,

$$a_2 \neq 0, \quad a_3 = \ldots = a_{2n+1} = 0, \quad a_{2n+2} \neq 0,$$

where a_2 is an arbitrary constant, which will be found by numerical methods, and a_{2n+2} is a constant depending on a_2 and f_n When $m \geq 2n+4$, a_m is found from,

$$a_m = \frac{1}{m(m-2)} \left(\sum_{i=2n}^{m-3} \sum_{j=n}^{i-1} f_j f_{i-j} a_{m-i-2} - \sum_{j=n}^{m-3} f_j f_{m-j-2} \right).$$

The asymptotic behaviour for $r \ll 1$ for $a(r)$ is,

$$a(r) \sim a_2 r^2 + a_{2n+2} r^{2n+2} \ldots$$

The behaviour for $r \gg 1$ is examined now. In anticipation of finding exponentially decaying solutions, we linearise equation (5.45) in the function $A(r)$ about the asymptotic value $a(r) = 1$. The equation is,

$$r^2 A_{rr} - r A_r - r^2 A = 0,$$

independent of vorticity n, which has a modified Bessel function solution,

$$A(r) = rK_1(r).$$

This justifies the expectation that the gauge field decays exponentially to its asymptotic value.

Next we examine the function $f(r)$. The series solutions are substituted into equation (5.46) and for $m \leq 3n+1$, f_j is found to satisfy,

$$\sum_{j=n}^{3n+1}(j^2-n^2)f_j r^j + \frac{\lambda}{2}\sum_{j=n+2}^{3n+1} f_{j-2}r^j \quad + \\ 2n^2 \sum_{m=n+2}^{3n+1}\sum_{j=2}^{m-1} f_{m-j}a_j r^m \quad - \quad n^2 \sum_{m=n+4}^{3n+1}\sum_{q=4}^{m-1}\sum_{i=2}^{q-1} a_i a_{q-i} f_{m-q} r^m = 0.$$

It is found that $f_n \neq 0$ and $f_{n+1} = 0$ by inspection. For powers of $m \geq 3n+2$,

$$f_m = \frac{1}{n^2-m^2}\left(\frac{\lambda}{2}f_{m-2} + 2n^2\sum_{j=2}^{m-1} f_{m-j}a_j - n^2\sum_{q=4}^{m-1}\sum_{i=2}^{q-1} a_i a_{q-i} f_{m-q} - \right. \\ \left. \frac{\lambda}{2}\sum_{p=2n}^{m-3}\sum_{i=n}^{p-1} f_i f_{p-i} f_{m-p-2}\right).$$

The asymptotic behaviour for $r \ll 1$ for $f(r)$ is,

$$f(r) \sim f_n r^n + f_{n+2}r^{n+2}\ldots,$$

where f_n is an arbitrary constant, which will be found by numerical methods, and f_{n+2} depends on a_2 and f_n.

The behaviour for $r \gg 1$ is examined now. In anticipation of finding exponentially decaying solutions, the equation (5.46) is linearised in the function $F(r)$ about the asymptotic value $f(r) = 1$. The equation is,

$$r^2F_{rr} + rF_r - 2\lambda r^2 F = 0,$$

independent of vorticity n, which has a modified Bessel function solution,

$$F(r) = K_0(\sqrt{2\lambda}r).$$

This justifies the expectation that the Higgs field decays exponentially to its asymptotic value, so that the static topological vortices of this system decay exponentially.

The behaviour of $h(r)$ is now examined in the regions $r \ll 1$ and $r \gg 1$. When the series solutions for $f(r)$ and $h(r)$ are substituted into equation (5.47) the result is;

$$\sum_{m=-k}^{\infty} \left(m^2 - k^2\right) h_m r^m - \sum_{m=2n-k+2}^{\infty} \sum_{p=0}^{m-3} \sum_{i=-n}^{p-1} f_{m-p-2} f_{p-i} h_i r^m = 0. \qquad (5.48)$$

If $0 < k \leq n$ then the coefficients satisfy,

$$h_{-k} \neq 0, \;\; h_{-k+1} = \ldots = h_{k-1} = 0, \;\; h_k \neq 0, \;\; h_{k+1} = 0 \ldots = h_{2n-k+1} = 0.$$

For $m \geq 2n - k + 2$ the coefficients satisfy,

$$h_m = \frac{1}{m^2 - k^2} \left(\sum_{p=n-k}^{m-3} \sum_{i=-k}^{p-1} f_{m-p-2} f_{p-i} h_i \right).$$

In this section we will show that there are $2n$ zero modes, that is that there are $2n$ terms in the Fourier expansion of $h(r, \theta)$. We show firstly that $k > n$ is not permitted as a possible zero mode. Assume that it is. Then the usual behaviour of $h_k(r)$ near the origin is,

$$h_k \sim \frac{c_1}{r^k} + c_2 r^k. \qquad (5.49)$$

In order that $\delta\phi$ be nonsingular, $h_k(r)$ must at most have an n'th order singularity at the origin. We will now show that all exponentially decreasing solutions at infinity lead to solutions with $c_1 \neq 0$. Assuming the contrary, we have, if $k > n$, then c_1 must be zero to ensure that $\delta\phi$ is regular at the origin. Consider the case of c_1 being zero, so that $h_k(r)$ behaves as,

$$h_k(r) \sim c_2 r^k, \qquad (5.50)$$

with $c_2 > 0$, since we are interested in positive $h_k(r)$. The function $h_k(r)$ is zero at the origin and initially increases. From the condition of finite energy the function $h_k(r) \to 0$ as $r \to \infty$, so that it must have a maximum at some r_0, and at this point,

$$\frac{d}{dr} h_k(r_0) = 0, \;\; \frac{d^2}{dr^2} h_k(r_0) \leq 0. \qquad (5.51)$$

However from equation (5.47), we have that the second derivative of h_k is positive at r_0, which leads to a contradiction. We now have that $c_1 \neq 0$. This excludes the possibility that $k > n$ because of the requirement of finite energy solutions.

We now have to exclude the possibility that $k = 0$. In this case $h_0(r)$ is regular at the origin and,

$$h_0 \sim A + Br^{2n+2}. \tag{5.52}$$

However this mode is not acceptible for the following reasons. Consider the equation (5.47) multiplied by $rh(r)$ and integrated by parts to obtain,

$$\int_0^\infty dr\, r \left[\left(\frac{dh_k}{dr} \right)^2 + \left(f^2 + \frac{k^2}{r^2} \right) h_k^2 \right] = r h_k \left. \frac{dh_k}{dr} \right|_{r=0}^{r=\infty}. \tag{5.53}$$

It can be seen that if $h_0(r)$ satisfies (5.52), then the right hand side of the equation (5.53) vanishes. The integral left is positive definite, and it is equal to zero, so that $h(r)$ is equal to zero. The only nonsingular solution with acceptible boundary conditions is the trivial one in the case of $k = 0$. Thus there are $2n$ acceptible solutions, those for which $1 \leq k \leq n$.

Chapter 6

The global existence of Abelian Yang-Mills solutions

6.1 Introduction

The purpose of this chapter is to formulate the Euler Lagrange equations as a Cauchy problem, that is a set of first order differential equations for which initial data can be specified. The solutions to the equations of motion are written in the form of a backround field added to a time dependent field. The static backround field and the time dependent field must satisfy certain conditions from [19], which guarantee the global existence of time dependent solutions. We will then examine the scattering of n vortices from each other.

6.2 Global existence

Euler-Lagrange equations for the Abelian Higgs model are equations (5.2) and (5.3) from the previous chapter, which are repeated here for convenience,

$$D_\mu D^\mu \Phi + \frac{\lambda}{2}\Phi(|\Phi|^2 - 1) = 0 \tag{6.1}$$

$$\partial_\mu F^{\mu\nu} + \frac{i}{2}(\Phi^*(D^\nu\Phi) - \Phi(\overline{D^\nu\Phi}) = 0. \tag{6.2}$$

The fields are written down in the form of a backround field and subtracted fields,

$$\Phi = \hat{\phi}(\vec{x}) + \psi(t,\vec{x}) \tag{6.3}$$
$$A_\mu = \hat{A}_\mu(\vec{x}) + a_\mu(t,\vec{x}). \tag{6.4}$$

The subtracted fields will lie in certain Sobolev spaces. It has been shown that a solution to the static Euler-Lagrange equations exists describing $n-$vortices superimposed at the origin, it is,

$$\hat{A}_0 = 0 \tag{6.5}$$
$$\hat{A}_i(r,\theta) = -\epsilon_{ij}x^j\frac{na(r)}{r^2} \tag{6.6}$$
$$\hat{\phi}(r,\theta) = f(r)\exp(in\theta) \tag{6.7}$$

The field configuration chosen as the backround field is the static $n-$vortex solution. In order that the time dependent equations of motion have solutions which exist globally, we impose conditions from [19]. These are

$$\hat{A}_0 = \partial_0\hat{A}_i = \partial_0\hat{\phi} = 0, \text{ and } \partial_i\hat{A}_i = 0, \ i = 1,2$$

$$\begin{aligned} \sup_{x\in\mathbf{R}^2} |\underbrace{\partial_i\ldots\partial_j\hat{A}_i}_{m-1}| &< \infty, \\ \sup_{x\in\mathbf{R}^2} |\underbrace{\partial_i\ldots\partial_j\hat{\phi}}_{m}| &< \infty, \ m = 0,1,2, \end{aligned} \tag{6.8}$$

$$(|\hat{\phi}|^2 - 1) \in L^2, \quad \hat{\nabla}_i\hat{\phi} := \partial_i\hat{\phi} - i\hat{A}_i\hat{\phi} \in \mathcal{H}_2$$
$$\hat{F}_{ij} \in \mathcal{H}_2, \quad \partial_i^2\hat{A}_j \in \mathcal{H}_1.$$

The Sobolev space of distributions with finite norm, $\mathcal{H}_s$, are defined by,

$$\| f \|^2_{\mathcal{H}_s} = \sum_{i+\ldots+j\leq s} \| \partial_i\ldots\partial_j f \|^2_{L^2} . \tag{6.9}$$

Here $\mathcal{H}_0$ denotes L^2. These conditions are chosen in order that the Cauchy problem which we will formulate as an integral equation, is a contraction mapping. This is an important step in the proving that the problem has a global solution $\psi : [0,\infty) \to \mathcal{H}_2$. See [19] for further details.

That these conditions hold can be seen by checking the asymptotic behaviour of the fields. The fields decay fast enough at infinity and are smooth. In [19] these conditions and conditions later imposed on initial data were used to establish bounds necessary to ensure global existence of the solution. The following functions are chosen as initial data,

$$\begin{aligned}
\psi(0,\vec{x}) &= 0, \\
a_\mu(0,\vec{x}) &= 0, \\
\partial_t\psi(0,\vec{x}) &= ne^{in\theta}f(r)h(r,\theta), \\
\partial_t a_0 &= 0, \\
\partial_t a_1(0,\vec{x}) &= \frac{n}{r}(-\sin\theta b(r,\theta)+\cos\theta c(r,\theta)), \\
\partial_t a_2(0,\vec{x}) &= \frac{n}{r}(\cos\theta b(r,\theta)+\sin\theta c(r,\theta)).
\end{aligned}$$

The following definitions have been made, which follow from the analysis of the zero modes studied in the previous chapter. The function $h(r,\theta)$ is defined by,

$$h(r,\theta)=\sum_{k=1}^{n}\left(h_k^{(1)}\cos k\theta + h_k^{(2)}\sin k\theta\right)$$

where the $h_k^{(i)}$, for $i=1,2$, may be complex functions. From the previous chapter we have for $b(r,\theta)$ and $c(r,\theta)$,

$$\begin{aligned}
b(r,\theta) &= -r\frac{\partial \mathrm{Re}\ h}{\partial r}+\frac{\partial \mathrm{Im}\ h}{\partial\theta} \\
c(r,\theta) &= r\frac{\partial \mathrm{Im}\ h}{\partial r}+\frac{\partial \mathrm{Re}\ h}{\partial\theta},
\end{aligned}$$

using the Fourier decomposition of the function $h(r,\theta)$ gives,

$$\begin{aligned}
b(r,\theta) &= \frac{1}{2}\sum_{k=1}^{n}\Big[(k\mathrm{Im}\ h_k^{(2)}-r\frac{d}{dr}(\mathrm{Re}\ h_k^{(1)}))\cos k\theta && (6.10)\\
&- (r\frac{d}{dr}(\mathrm{Re}\ h_k^{(2)})+k\mathrm{Im}\ h_k^{(1)})\sin k\theta\Big] && (6.11)\\
c(r,\theta) &= \frac{1}{2}\sum_{k=1}^{n}\Big[(k\mathrm{Re}\ h_k^{(2)}+r\frac{d}{dr}(\mathrm{Im}\ h_k^{(1)}))\cos k\theta && (6.12)\\
&+ (r\frac{d}{dr}(\mathrm{Im}\ h_k^{(2)})-k\mathrm{Re}\ h_k^{(1)})\sin k\theta\Big]. && (6.13)
\end{aligned}$$

For the time dependent field,

$$\begin{aligned} \Psi^T(t,\vec{x}) &= (a_0, p_0, a_1, p_1, a_2, p_2, \psi, \pi^*) \\ \text{where } p_\mu := \partial_0 a_\mu \quad &, \quad \text{and } \pi^* := \partial_0 \psi - i a_0 \psi, \end{aligned}$$

the initial data satisfy,

$$\psi \in \mathcal{H}^{(s)} := (\mathcal{H}_{s+1} \times \mathcal{H}_s)^4, s \geq 0.$$

The expansion of the fields in terms of a static backround field and dynamic field is substituted into the Euler Lagrange equations. The zeroth component of equation (6.2) is the Gauss law constraint, which reads,

$$-\Delta a_0 + \partial_0 \partial_i a_i = -\frac{i}{2}\left((\hat{\phi}^* + \hat{\psi}^*)(\pi^* - i a_0 \hat{\phi}) - (\hat{\phi} + \hat{\psi})(\pi^+ i a_0 \hat{\phi}^*)\right).$$

In this equation, no use has been made of the Lorentz gauge condition,

$$\partial_\mu a_\mu = 0.$$

Both the Lorentz condition and the Gauss law hold at $t = 0$. In reference [19] it is shown that these conditions propagate, and hence hold for all time. The use of the Lorentz condition and the Gauss law gives a second order partial differential equation for a_0.

When the other components of equation (6.2) and equation (6.1) are expanded, the result is a set of four second order differential equations. These can be written as a set of 8 first order equations,

$$\frac{d}{dt}\Psi = -i\tilde{A}\Psi + J, \tag{6.14}$$

The operator $\tilde{A}$ is defined by,

$$\tilde{A} = i \begin{pmatrix} \Gamma & 0 & 0 & 0 \\ 0 & \Gamma & 0 & 0 \\ 0 & 0 & \Gamma & 0 \\ 0 & 0 & 0 & \Gamma \end{pmatrix} \quad , \Gamma = \begin{pmatrix} 0 & 1 \\ \Delta - m^2 & 0 \end{pmatrix}, \tag{6.15}$$

where

$$m^2 > 0, \ \Delta = \partial_i^2, \ \nabla_i := \partial_i - i a_i.$$

The vector J has components, $J_1 = 0 = J_{2i+1}$ for $i = 1, 2$, the nonzero components are calculated as,

$$J_2 = m^2 a_0 - \frac{i}{2}\left((\hat{\phi}^* + \hat{\psi}^*)\pi^* - (\hat{\phi} + \hat{\psi})\pi\right) - \frac{a_0}{2}(\hat{\phi}\psi^* + 2 \parallel \hat{\phi} \parallel^2 + \hat{\phi}^*\psi)$$

$$\begin{aligned}
J_{2i+2} &= -\frac{i}{2}\left[\hat{\phi}^*\hat{\nabla}_i\hat{\phi} - \hat{\phi}(\hat{\nabla}_i\hat{\phi})^*\right] + m^2 a_i + \Delta\hat{A}_i - \frac{i}{2}\left[\psi^*\hat{\nabla}_i\hat{\phi} - \psi(\hat{\nabla}_i\hat{\phi})^*\right] \\
&- \frac{i}{2}\left[(\hat{\phi}^* + \psi^*)(\nabla_i\psi) - (\hat{\phi} + \psi)(\nabla_i\psi)^*\right] \\
&- \frac{1}{2}\left[(\hat{\phi}^* + \psi^*)(\hat{A}_i\psi + a_i\hat{\phi}) - (\hat{\phi} + \psi)(\hat{A}_i\psi^* + a_i\hat{\phi}^*)\right], \text{ for } i = 1, 2, \\
J_7 &= ia_0\psi \\
J_8 &= m^2\psi - i\partial_i(\hat{A}_i\hat{\phi}) - i\hat{A}_i\hat{\nabla}_i\hat{\phi} + ia_0\pi^* + \Delta\hat{\phi} - i\partial_i(a_i\psi) - ia_i\nabla_i\psi \\
&- 2ia_i\hat{\nabla}_i\hat{\phi} - 2i\hat{A}_i\nabla_i\psi + ip_0\pi^* - i(\partial_i a_i)\hat{\phi} - A_i A_i + a_\mu a^\mu \\
&- \frac{1}{2}\left[\psi(\parallel \hat{\phi} + \psi \parallel^2 - 1) + \hat{\phi}(\parallel \hat{\phi} \parallel^2 - 1) + \hat{\phi}(\hat{\phi}\psi + \hat{\phi}^*\psi + \parallel \psi \parallel^2)\right].
\end{aligned}$$

The next step is to test the conditions of the existence proof, and to check that the initial data chosen conforms to the requirements. It is obvious that

$$\hat{A}_0 = \partial_0\hat{A}_i = \partial_0\hat{\phi}_i = 0,$$

and

$$\partial_i\hat{A}_i = 0.$$

From the previous chapter and Plohr [20], it is known that the functions $a(r)$ and $f(r)$ decay exponentially as $r \to \infty$ to their asymptotes. The behaviour at the origin is also known,

$$\begin{aligned}
a(r) &\sim a_2 r^2 + a_{2n+2} r^{2n+2} \ldots \\
f(r) &\sim f_n r^n + f_{n+2} r^{n+2} \ldots .
\end{aligned}$$

The functions $h_k^{(i)}$ $i = 1, 2$ in the Fourier expansion were shown to behave as,

$$h = h_{-k} r^{-k} + h_k r^k + \ldots$$

at the origin and decay exponentially as $r \to \infty$. These properties guarantee that the conditions hold. The energy at $t = 0$ is finite and is equal to the lower bound derived in the previous chapter. This is because the static solutions were chosen to solve the Bogomolny'i equations. The conditions of the paper [19] are shown to have been fulfilled and so there exists a global finite energy solution to the Cauchy problem.

6.3 Rotation Symmetries

In this section we will discuss the symmetries of the solution to the Cauchy problem. It will be shown that for a particular choices of initial data, the solution has symmetries which will propagate. We take as the first example the scattering of n vortices, [21]. This will serve as a model for the examination of further scattering processes.

The initial data chosen for the problem are,

$$\begin{aligned}
\psi(0,\vec{x}) &= 0 \\
a_\mu(0,\vec{x}) &= 0 \qquad (6.16)\\
\partial_t\psi(0,\vec{x}) &= ne^{in\theta}f(r)h(r,\theta) \qquad (6.17)\\
\partial_0 a_1(0,\vec{x}) &= -n\sin((n-1)\theta)\left(\frac{rh'(r)+nh(r)}{r}\right)\\
\partial_0 a_2(0,\vec{x}) &= -n\cos((n-1)\theta)\left(\frac{rh'(r)+nh(r)}{r}\right).
\end{aligned}$$

The function $h(r)$ satisfies the differential equation,

$$r^2h''(r)+rh'(r)-h(r)(n^2+r^2f^2(r))=0. \qquad (6.18)$$

The solution for the Cauchy problem (6.14) is written as the solution of the following integro-differential equation,

$$\Psi(t,\vec{x}) = e^{-i\tilde{A}t}\Psi(0,\vec{x}) + \int_0^t ds\exp[-i\tilde{A}(t-s)]J(\Psi(s,\vec{x})). \qquad (6.19)$$

In turn this integro-differential equation is solved by the limit of a sequence of successive approximations Ψ_n defined by the formula:

$$\Psi_{n+1}(t,\vec{x}) = e^{-i\tilde{A}t}\Psi(0,\vec{x}) + \int_0^t ds\exp[-i\tilde{A}(t-s)]J(\Psi_n(s,\vec{x})), \qquad (6.20)$$

where $\Psi_0 = \Psi(0,\vec{x})$, with the initial data (6.17). We now establish certain symmetries of the initial data Ψ_0 and use (6.20) to establish these symmetries for the successive approximations Ψ_n, and finally for the solution of (6.14).

The first transformation we study is $\vec{x}\to\vec{x}' = S\vec{x}$ where S is the orthogonal matrix

$$S = \begin{pmatrix} \cos\frac{2\pi}{n} & -\sin\frac{2\pi}{n} \\ \sin\frac{2\pi}{n} & \cos\frac{2\pi}{n} \end{pmatrix} \qquad (6.21)$$

Under this transformation the initial data change as follows:

$$\Psi(0,\vec{x}') = M_1\Psi(0,\vec{x}),$$

with

$$M_1 = \begin{pmatrix} I & 0 & 0 & 0 \\ 0 & A & -B & 0 \\ 0 & B & A & 0 \\ 0 & 0 & 0 & I \end{pmatrix} \ , \ I = \begin{pmatrix} 1 & 0 \\ 0 & 1 \end{pmatrix} \ , A = \cos\frac{2\pi}{n}I \ , \ B = \sin\frac{2\pi}{n}I. \tag{6.22}$$

We can see that $J(M_1\Psi(s,\vec{x})) = M_1 J(\Psi(s,\vec{x}))$, $[M_1,\tilde{A}] = 0$ and

$$\exp(-i\tilde{A}t)M_1\Psi_n(s,\vec{x}) = M_1\exp(-i\tilde{A}t)\Psi_n(s,\vec{x}),$$

which implies that $\Psi_n(t,\vec{x}') = M_1\Psi_n(t,\vec{x})$ for all $n \in \mathcal{N}$. From this follows $\Psi(t,\vec{x}') = M_1\Psi(t,\vec{x})$ for the solution Ψ.

Next we study the reflection $(x_1,x_2) \to (x_1,-x_2)$. Under this transformation the initial data change as follows: $\psi(t,x_1,-x_2) = M_2\psi(t,x_1,x_2)$, where

$$M_2 = \begin{pmatrix} -I & 0 & 0 & 0 \\ 0 & -I & 0 & 0 \\ 0 & 0 & I & 0 \\ 0 & 0 & 0 & C \end{pmatrix} \ , \ CV = V^* \tag{6.23}$$

Furthermore, $J(M_2\Psi(s,\vec{x})) = M_2 J(\Psi(s,\vec{x}))$. Again we have $[M_2,\tilde{A}] = 0$, and $\Psi_n(t,x_1,-x_2) = M_2\Psi_n(t,x_1,x_2)$. From this follows $\Psi(t,x_1,-x_2) = M_2\Psi_n(t,x_1,x_2)$, for the solution Ψ.

Under the transformations considered, all terms in the energy density:

$$\mathcal{E} = \frac{1}{2} \mid D_0\Phi \mid^2 + \frac{1}{2} \mid D_i\Phi \mid^2 + \frac{1}{4}F_{ij}^2 + \frac{1}{2}F_{0i}^2 + \frac{\lambda}{8}(\mid \Phi \mid^2 - 1)^2, \tag{6.24}$$

are invariant. This leads to the following conclusion: If by using functions like $\mid \Phi \mid^2$,F_{ij}^2 or $\mathcal{E}$, there is a way of defining the positions $(x_1^a(t),x_2^a(t)), a = 1,2$, of exactly n separate vortices, these n positions must lie on n radial lines separated by an angle $\frac{2\pi}{n}$ with equal distance from the origin. (Below we will use the the minima of $\mid \Phi \mid^2$ to define these positions.) Furthermore, one of these radial lines must be the positive x_1-axis, or make an angle $\frac{\pi}{n}$ with the positive x_1-axis. Any vortex that does not satisfy these conditions

immediately leads to $2n-1$ other vortices, because of the symmetries of our solution. Since our solution is continuous, these positions will change continuously such that at $t=0$ the n positions coincide, and after the collision the vortices move again on the radial lines just described. Therefore, they can either go back on the radial lines they came in on, or go back on radial lines shifted by an angle $\frac{\pi}{n}$. We will study a further symmetry and use the Cauchy-Kowalewskyi theorem [22] to show that the second case is realised.

The last transformation we study is $\vec{x} \to M\vec{x}$ where M is the orthogonal matrix

$$M = \begin{pmatrix} \cos\frac{\pi}{n} & -\sin\frac{\pi}{n} \\ \sin\frac{\pi}{n} & \cos\frac{\pi}{n} \end{pmatrix}. \tag{6.25}$$

Under this transformation the initial data change as follows:

$$\Psi(0, M\vec{x}) = M_3\Psi(0, \vec{x}),$$

with

$$M_3 = \begin{pmatrix} -\sigma & 0 & 0 & 0 \\ 0 & C & -D & 0 \\ 0 & D & C & 0 \\ 0 & 0 & 0 & -\sigma \end{pmatrix}, \ \sigma = \begin{pmatrix} 1 & 0 \\ 0 & -1 \end{pmatrix}, C = \cos\frac{\pi}{n}\sigma, \ D = \sin\frac{\pi}{n}\sigma. \tag{6.26}$$

We can see that $J(M_3\Psi(s,\vec{x})) = -M_3J(\Psi(s,\vec{x}))$, $\{M_3, \tilde{A}\} = 0$ and

$$\exp(i\tilde{A}t)M_3 = M_3\exp(-i\tilde{A}t).$$

From this follows $\Psi(-t, M\vec{x}) = M_3\Psi(t,\vec{x})$, and we see that all terms in the energy density are invariant under the transformation $(t,\vec{x}) \to (-t, M\vec{x})$. This establishes $\frac{\pi}{n}$ scattering for n vortices. To show that, for small time t, $|\Phi|$ has exactly n minima (so that we can identify n vortices), we use the Cauchy-Kowalewskyi theorem [22] .

From Ref [20], we know that f starts with an r^n term and a starts with an r^2 term. Equation (6.18) shows that asymptotically near $r=0$,

$$k \sim k_{-n}r^{-n} + k_n r^n. \tag{6.27}$$

Using the same techniques as in Ref [23], we can now establish the analyticity of the initial data, and verify that all the conditions of the Cauchy-

Kowalewskyi theorem [22] are satisfied. We therefore have an analytic solution near the origin. This solution leads to the following asymptotic expression for $|\Phi|^2$:

$$|\Phi|^2(t,\vec{x}) \sim f_n^2(x_1^2+x_2^2)^n + 2ntf_n^2k_{-n}\sum_{p=0}^{[n/2]}(-1)^{n+p}\left(\begin{array}{c} n \\ 2p \end{array}\right)x_1^{n-2p}x_2^{2p} + Kt^2, \tag{6.28}$$

where we have assumed that x_1 and x_2 are of order ϵ, and t is of order ϵ^n, so that higher order terms can be ignored. (K is a constant that can be expressed in terms of the coefficients of the expansions of a, f, and k. $[n/2]$ is the highest integer that does not exceed $n/2$.) For $t \neq 0$, the approximation (6.28) of $|\Phi|^2$ has exactly n minima which lie at $r = (n|t|k_{-n})^{1/n}$ and $\theta = 0, \frac{2\pi}{n}, ..., \frac{2(n-1)\pi}{n}$ for $t < 0$, and at $r = (n|t|k_{-n})^{1/n}$ and $\theta = \frac{\pi}{n}, \frac{3\pi}{n}, ..., \frac{(2(n-1)+1)\pi}{n}$ for $t > 0$. This establishes the $\frac{\pi}{n}$ symmetry of the process. Our rigorous method is, however, not capable of following the minima for large time t.

Chapter 7

Dynamics of Abelian Higgs vortices.

7.1 Introduction

In this section the properties of the zero modes are discussed. From the Refs. [18] and [24], it is known that the zero modes of a static configuration of $n-$ vortices can be infinitesimally deformed. This deformation allows one to place $n-$ vortices at arbitrary points on the plane. This static configuration depends on $2n$ parameters. In a previous chapter we have shown that a judicious choice of the zero modes for initial data for the Cauchy problem, will have the correct symmetries for the solution to exhibit π/n scattering of $n-$vortices.

7.2 Zero Modes

The zero modes of the Bogomol'nyi equations of the Abelian Higgs model arise as a result of fluctuations. This is discussed in a previous chapter. The reason for studying these is as follows. In the Bogomol'nyi limit of the Abelian Higgs model the energy momentum tensor has vanishing diagonal components. It follows that there is no interaction between static vortices as was discussed in [12]. It has also been shown that the energy of the vortices is at its minimum value. It is possible to place single vortices at arbitrary points in the plane and study their properties.

For convenience we rewrite the Bogomol'nyi equations,

$$(D_1 + iD_2)\Phi, \quad F_{12} = \frac{1}{2}(|\Phi|^2 - 1).$$

The Ansatz used for the functions A_i and Φ was substituted into these equations in the previous chapter. The function $h(r,\theta)$ is found to be of the form,

$$h(r,\theta) = \sum_{k=1}^{n} \left(h_k^{(1)}(r) \cos k\theta + h_k^{(2)}(r) \sin k\theta \right), \tag{7.1}$$

and the equation satisfied by $h_k^{(i)}$ is,

$$\frac{1}{r}\frac{d}{dr}\left(\frac{dh_k^{(i)}}{dr}\right) - \left(f^2 + \frac{k^2}{r^2}\right) h_k^{(i)} = 0. \tag{7.2}$$

The functions $b(r,\theta)$ and $c(r,\theta)$ were defined in terms of differential equations involving $h(r,\theta)$ and are defined here in terms the series for $h(r,\theta)$,

$$\begin{aligned} b(r,\theta) &= -r\frac{\partial}{\partial r}\mathrm{Re}\ h + \frac{\partial}{\partial\theta}\mathrm{Im}\ h & (7.3)\\ &= \sum_{k=1}^{n}\left[\left(k\mathrm{Im}\ h_k^{(2)} - r\frac{d}{dr}\mathrm{Re}\ h_k^{(1)}\right)\cos k\theta - \right. & (7.4)\\ &\quad \left.\left(k\mathrm{Im}\ h_k^{(1)} + r\frac{d}{dr}\mathrm{Re}\ h_k^{(2)}\right)\sin k\theta\right], & (7.5) \end{aligned}$$

and $c(r,\theta)$ is given similarly,

$$\begin{aligned} c(r,\theta) &= r\frac{\partial}{\partial r}\mathrm{Im}\ h + \frac{\partial}{\partial\theta}\mathrm{Re}\ h & (7.6)\\ &= \sum_{k=1}^{n}\left[\left(k\mathrm{Re}\ h_k^{(2)} + r\frac{d}{dr}\mathrm{Im}\ h_k^{(1)}\right)\cos k\theta + \right. & (7.7)\\ &\quad \left.\left(-k\mathrm{Re}\ h_k^{(1)} + r\frac{d}{dr}\mathrm{Im}\ h_k^{(2)}\right)\sin k\theta\right]. & (7.8) \end{aligned}$$

7.3 Minima of the Higgs field

In this section approximations to the minima of the modulus of the Higgs field are considered. To first order in the expansion parameter, α, the Higgs

and gauge fields are given by,

$$\Phi = \hat{\phi} + \alpha\zeta \tag{7.9}$$
$$A_i = \hat{A}_i + \alpha a_i. \tag{7.10}$$

where

$$\hat{\phi} = f(r)\exp(in\theta), \quad \zeta = nf(r)h(r,\theta)\exp(in\theta), \tag{7.11}$$
$$h(r,\theta) = \sum_{k=1}^{n} \tilde{h}_k(r)\exp(-ik\theta). \tag{7.12}$$

Using these functions, an approximation to the modulus of the Higgs field is calculated as,

$$|\Phi|^2 = f^2(1 + \alpha n(h(r,\theta) + h^*(r,\theta)) + \alpha^2 n^2 |h(r,\theta)|^2). \tag{7.13}$$

The static solutions satisfy the Bogomol'nyi equtions, and hence the Euler-Lagrange equations. Then sum of the static solution and a linear combination of the fluctuations will be a solution of the linearized Euler Lagrange equations. This is the basis for the approximation of the modulus of the Higgs field. There is a $2n$ parameter family of solutions which are the linear fluctuations of the Bogomol'nyi equations.

7.4 Arbitrarily positioned vortices

Consider the $2n$ parameters defining the positions of the vortices, in polar coordinates. This is a set of n couples (θ_i, r_i) We chose the most symmetrical form for the vortices; they are placed on a circle of radius $r = r_0$. Theorem 1.1 of Ref. [24] states: Given an integer $n \geq 0$ and a set $\{z_i\}, j = 1, 2, \ldots, n$ of n points in $\mathbf{C}$, there exists a finite action solution to the Bogomol'nyi equations, unique up to gauge equivalence, with the following properties. 1) The solution is globally C^∞. 2) The set of zeroes of Φ are the set of points $\{z_j\}$. Further, the behaviour of the Higgs field is given as,

$$z \to z_j, \quad \Phi \sim c_j(z - z_j)^{n_j}, \quad c_j \neq 0,$$

where n_j is the multiplicity of z_j in the set $\{z_j\}$. The positions of the vortices occur at the zeroes of the Higgs field. In the approximation to be constructed,

we will consider the minima of the modulus of the Higgs field to be the locations of the vortices. The Higgs field is given by,

$$\Phi = f(r)\exp[in\theta] + \alpha n f(r)h(r,\theta)\exp[in\theta], \tag{7.14}$$

$$h(r,\theta) = \sum_{k=1}^{n} \alpha_k \tilde{h}_k \exp[-ik\theta], \tag{7.15}$$

the approximation to the modulus is given by, $Q(r,\theta) = |\Phi|^2$,

$$Q(r,\theta) = f^2(1 + 2\alpha \mathrm{Re}\ (h) + \alpha^2 n^2 h h^*) \tag{7.16}$$

$$= f^2(1 + 2\alpha n \sum_{k=1}^{n} \mathrm{Re}\ (\alpha_k \tilde{h}_k \exp(-ik\theta)) + \tag{7.17}$$

$$\alpha^2 n^2 \sum_{k=1}^{n}\sum_{m=1}^{n} \alpha_k \alpha_m^* \tilde{h}_k \tilde{h}_m \exp[-i(k-m)\theta]). \tag{7.18}$$

Specify n vortices in the plane with positions, $z_k = r_k e^{i\theta_k}$, where θ_k are the arguments of the position of the k'th vortex, and r_k is its distance from the origin. For simplicity, let all the vortices lie on a circle, so that $r_k = r_0$ $\forall k, 1 \leq k \leq n$. The function $Q(r,\theta)$ has $2n$ unknown numbers, the α_k,

$$\alpha_k = \mathrm{Re}\ (\alpha_k) + i\mathrm{Im}\ (\alpha_k).$$

The minima of the modulus of the Higgs field are where the vortices are positioned. Consider the condition on the following partial derivatives,

$$\left.\frac{\partial}{\partial\theta}Q\right|_{\theta=\theta_j, r=r_0} = 0, \quad \left.\frac{\partial}{\partial r}Q\right|_{\theta=\theta_j, r=r_0} = 0.$$

These relations give $2n$ equations for $2n$ unknowns. The numerical solution to these equations has been found. The solution is a set of n numbers, α, with real and complex parts, giving the $2n$ parameters required.

The following are graphs plotted using this approximation to the modulus of the Higgs field. There are contour plots of the function $Q(r,\theta)$. Leading terms in the series approximations of the functions $f(r), a(r)$ and $\tilde{h}_k(r)$ were used. These were discussed in previous chapters. The plots of the energy density were calculated using numerical solutions of the static one dimensional Euler-Lagrange equations. Numerical methods were used

to approximate these functions. In particular, a fourth order Runge-Kutta integration scheme implemented in C was used, and routines from Ref. [25]. The shooting method was employed, this ensures the correct behaviour of the fields at the boundary conditions is respected. The code was written so as to minimize the difference between the numerical solution and its asymptote. It is an iterative process.

Because the equations are singular at the origin integration must begin at a finite distance way from the origin $r_0 > 0$. Taylor series of the solutions provide approximations to the initial data at r_0. The integration procedes to some finite value, r_∞, where the integration was stopped. The choice of r_∞ is made from consideration of the difference of the solution from the boundary values. The differential equations can be considered to be of the form,

$$\frac{df_i}{dr} = J_i(f_1, f_2, \ldots). \tag{7.19}$$

The shooting method was implemented to minimize the distance of the solution to the asymptotes, that is,

$$\sum_i \left(f_i(r_\infty - \lim_{r\to\infty} f_i(r) \right)^2. \tag{7.20}$$

The value of (7.20) varies for the different problems from 10^{-6} to 10^{-10}.

The programs written in C language were solved in double precision accuracy, with step sizes of $h = 0.005$. The calculations were started with step sizes of $h = 0.1$ and $h = 0.01$ and decreased until there was no change in the form of the solution. Some of the C programmes had an adaptive grid scheme which decreased the step size automatically. These provided the best results.

The shooting method was also implemented in "Mathematica". This programme uses a one step Euler scheme to integrate differential equations, but has an adaptive procedure to determine the step size. If the solution appears to be varying rapidly in a particular region, then the integration routine will reduce the step size to better track the solution. Accuracy parameters can be fixed to ensure truncation and roundoff errors are small. The number of precision digits in the internal computation of the solution was chosen to be 15 and the accuracy of such a solution was chosen to be 10 digits.

The value of (7.20) in the Mathematica calculations was found to be of order 10^{-10} and lower. Another criterion for acceptible numerical approximations, is to chose those for which the integral of the static energy density

is close to the Bogomol'nyi bound, but this is only valid for the self dual limit. Agreement with this criterion was found to vary from 10^{-4} to 10^{-7}. In the case of the Bogomol'nyi limit one of the free parameters can be evaluated from the series solution of the Bogomol'nyi equations. Again these numbers provided checks on the numerical calculations. There was good agreement between the two methods of integrating the differential equations.

Figure 7.1: Contour plot of the energy density for the $n = 3$ vortices ,$t < 0$. For all of the following plots, the gradient of colour from white to black represents a decrease in height.

Figure 7.2: Contour plot of the energy density for the $n = 3$ vortices ,$t = 0$.

Figure 7.3: Contour plot of the energy density for the $n = 3$ vortices ,$t > 0$.

Figure 7.4: Three dimensional plot of the energy density

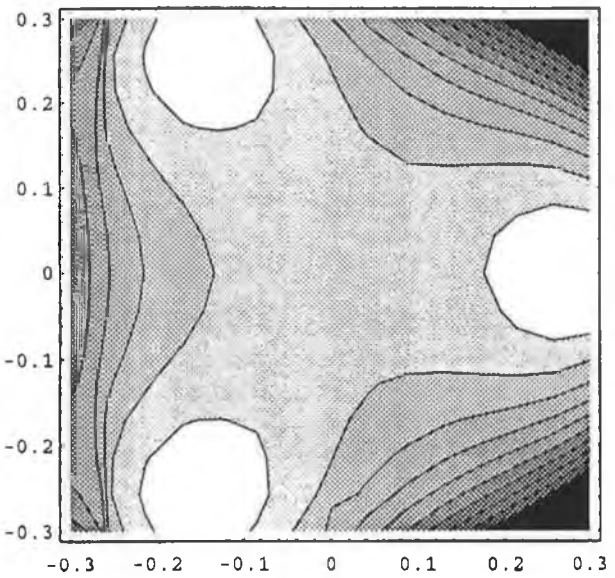

Figure 1

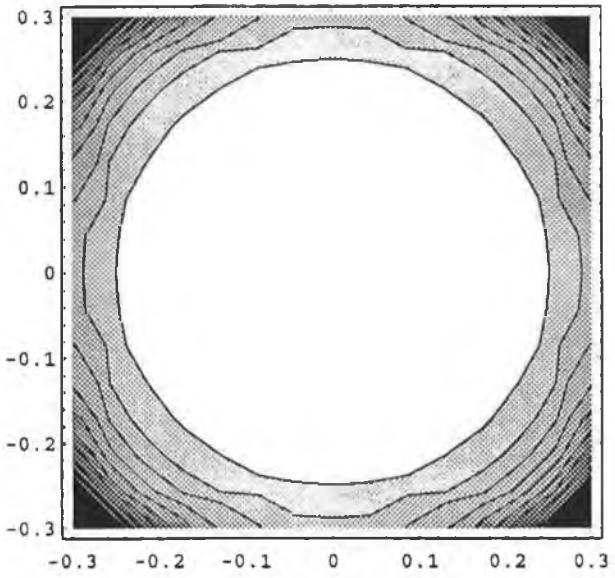

Figure 2

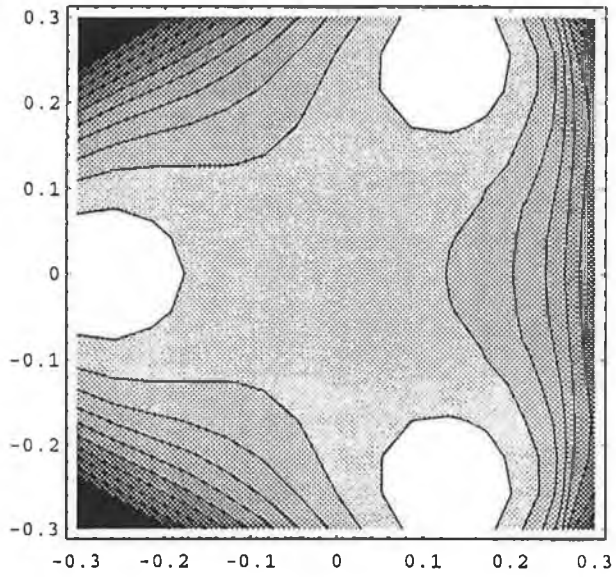

Figure 3

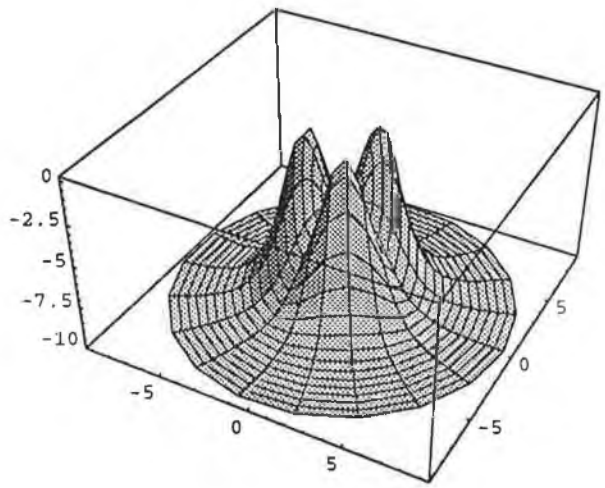

Figure 4

Chapter 8

Summary and Conclusions

Our results as given in previous chapters are presented and discussed. The fact that the models presented in this thesis are gauge theories, plays an important role in our search for vortex solutions. In a gauge theory solutions of the equations of motion can be transformed, using a transformation which may be different for each point in space-time, to new solutions, and the physics the solution describes is unaffected by this transformation. The first model we examined was the gauged $O(3)$ sigma model with a Maxwell term, whose Lagrangian is (2.1). The second model was the gauged $O(3)$ sigma model with a Chern-Simons term, whose Lagrangian is (3.1). Chern-Simons models may explain high temperature superconducting behaviour [2].

An important feature of these models is the special choice of potential motivated by our desire to find vortex solutions. Another important feature is that the models are gauge theories with gauge transformation,

$$\vec{\phi} \to \vec{\phi}' = O(t, \vec{x})\vec{\phi}, \tag{8.1}$$

and

$$A_\mu \to A'_\mu = A_\mu - \partial_\mu \theta, \tag{8.2}$$

where $O(t, \vec{x})$ is given by (2.3). This enables us to write down the ansatz (2.41), (2.42), which led to smooth solutions in this gauge. In another singular gauge, all of the ϕ^α are just radial functions. The gauge freedom gave us more flexibility in our search for solutions.

The third model studied was the Abelian Chern-Simons-Higgs model, with the Lagrangian (4.1). The fourth was the Abelian Yang-Mills-Higgs

model with the Lagrangian (5.1). The Lagrangian of the Ginzburg-Landau theory [1] which describes superconductors, is the static part of (5.1). Again, these models are gauge theories in the following sense. Under the $U(1)$ transformations,

$$\phi \to \phi' = \exp(i\alpha(\vec{x},t))\phi, \quad A_\mu \to A'_\mu = A_\mu - \partial_\mu \alpha, \tag{8.3}$$

the Lagrangian (5.1) is invariant. The Lagrangian with the Chern-Simons term gains a four divergence, but this does not effect the equations of motion. Again gauge transformations gave more freedom and here allowed us to write down a radially symmetric ansatz in the form (4.20).

The third aspect of our theories which played an important role was the nontrivial topology of finite energy configurations. In the case of both of the sigma models, we ensured finite energy configurations by imposing conditions on ϕ^3, namely,

$$\lim_{r\to\infty} \phi^3 = 1. \tag{8.4}$$

This followed from considering the potential, $V(|\phi^3|)$. As $r \to \infty$ in any direction the field $\vec{\phi}$ takes the same value. Thus the space $\mathbf{R}^2$ can be compactified and considered as $\mathbf{S}^2$. The three component field, $\vec{\phi}$ was viewed as a map from one sphere to another, because $\vec{\phi}$ is a 3 component vector of unit length and takes its values on a sphere.

In the case of the Abelian Chern-Simons-Higgs and Abelian Yang-Mills-Higgs models, we ensured finite energy configurations by also considering the potential. The asymptotic value of the complex field, Φ, had to satisfy

$$\lim_{r\to\infty} \Phi\Phi^* = 1. \tag{8.5}$$

The field Φ should be a unimodular complex number as $r \to \infty$. In this case the complex scalar field, Φ, was viewed as a map from the circle at infinity to the circle of unimodular complex numbers.

In both types of model, the solutions are characterised by an integer called the winding number, or vorticity. Configurations with different vorticities cannot be smoothly deformed into each other without violating the boundary conditions. The winding number for the sigma models is given by,

$$N = \frac{1}{8\pi} \int \epsilon_{ij}\epsilon^{abc}\partial_i\phi^a\partial_j\phi^b\phi^c. \tag{8.6}$$

It tells how many times the sphere is covered by the mapping $\vec{\phi}$. The winding number for the other models is given by,

$$N = \frac{1}{2\pi} \int \epsilon_{ij} \partial_i A_j, \tag{8.7}$$

indicating how many times the circle is covered.

The nontrivial topology of the space of finite energy configurations in all the models helped us to find solutions. We examined one sector of topologically nontrivial configurations and found one there with minimal energy, which was of course a solution. To implement this strategy, we used the following lower bounds,

$$\mathcal{H}_0 = \frac{1}{4} F_{ij}^2 + \frac{1}{2} (D_i \phi^a)^2 + \frac{\lambda_0}{2} (\phi^3 - 1)^2 \geq 2\pi N, \tag{8.8}$$

$$\mathcal{H}_0 = \frac{\kappa^2}{2} \frac{F_{ij}^2}{|\phi^\alpha|^2} + (D_i \phi^a)^2 + \frac{\lambda_0}{\kappa^2} (1 - \phi^3)^3 (1 + \phi^3) \geq 8\pi N, \tag{8.9}$$

$$\mathcal{H}_0 = \frac{F_{ij}^2}{|\Phi|^2} + (D_i \Phi)(\overline{D_i \Phi}) + \frac{\lambda_0}{8} |\Phi|^2 (1 - |\Phi|^2)^2 \geq 2\pi N, \tag{8.10}$$

$$\mathcal{H}_0 = \frac{1}{4} F_{ij}^2 + \frac{1}{2} (D_i \Phi)(\overline{D_i \Phi}) + \frac{\lambda_0}{8} (1 - |\Phi|^2)^2 \geq \pi N. \tag{8.11}$$

We next showed that it is possible to saturate the lower bound for one particular value of the coupling constant, λ_0, in the potential. Since the vortex number is a topological invariant, any configuration which achieves this lower bound is a minimum of the energy and thus a solution of the Euler-Lagrange equations. The corresponding fields satisfy a set of first order nonlinear partial differential equations, usually called Bogomol'nyi equations. To display their similarity, they are listed below in the order in which the models are given above.

$$F_{ij} = -\epsilon_{ij} (1 - \phi^3), \tag{8.12}$$

$$\epsilon_{ij} D_i \phi^a = \epsilon^{abc} D_j \phi^b \phi^c, \tag{8.13}$$

$$F_{ij} = -\epsilon_{ij} (1 - \phi^3)^2 (1 + \phi^3), \tag{8.14}$$

$$\epsilon_{ij} D_i \phi^a = \epsilon^{abc} D_j \phi^b \phi^c, \tag{8.15}$$

$$F_{12} = \frac{1}{4}|\Phi|^2(1-|\Phi|^2), \tag{8.16}$$

$$D_i\Phi = i\epsilon_{ij}D_j\Phi, \tag{8.17}$$

$$F_{12} = -\frac{1}{2}(|\Phi|^2-1), \tag{8.18}$$

$$(D_1+iD_2)\Phi = 0. \tag{8.19}$$

We used the Euler-Lagrange equations so that we could work with an arbitrary value of the coupling constant λ_0. We made the radially symmetric ansatz,

$$A_i = \frac{a(r)-N}{r}\epsilon_{ij}\hat{x}_j, \tag{8.20}$$

$$\phi^\alpha = \sin f(r)n^\alpha, \;\; \phi^3 = \cos f(r). \tag{8.21}$$

A gauge transformation can transform $\vec{\phi}$ to,

$$\vec{\phi} = (\sin f(r), 0, \cos f(r))^T, \tag{8.22}$$

which makes the radial symmetry clear, but in that gauge the solutions are not smooth. In the case of the Abelian Chern-Simons-Higgs and Abelian Yang-Mills-Higgs models, we employed the ansatz,

$$A_i = -\epsilon_{ij}\frac{nx_j}{r^2}a(r), \;\; \Phi = f(r)\exp(in\theta). \tag{8.23}$$

Again there is a gauge transformation transforming Φ to $\Phi = f(r)$, which makes the radial symmetry clear.

We assumed the potential energy density obeyed the same radially symmetric ansatz and found the Euler-Lagrange equations arising from the one dimensional subsystem. These equations were second order non-linear ordinary differential equations. A study of the asymptotic behaviour of the solutions was made at the origin and at infinity. Suitable conditions were found to ensure finite energy and numerical techniques were used to find solutions. We varied the coupling parameter in the potential and computed the integral of the energy density. This enabled us to produce graphs of the energy per unit vortex and see whether the vortices repeled or attracted.

In the next chapters we examined the dynamics of vortices in one particular model, the Abelian Yang-Mills-Higgs model. We used the Euler-Lagrange equations and formulated a Cauchy problem for the subtracted fields, Ψ,

$$\frac{d}{dt}\Psi = -i\tilde{A}\Psi + J. \tag{8.24}$$

We subtracted from the original fields topologically nontrivial background fields, because we wanted to put the subtracted fields into certain Sobolev spaces not containing topologically nontrivial fields. As background fields we took the static solutions of n superimposed vortices. At $t = 0$, the subtracted fields were zero and for their time derivatives we took the zero modes.

The zero modes are fluctuations which leave the potential energy unchanged, and so the Bogomol'nyi equations still hold. For n vortices it was shown that there is a $2n$ parameter family of solutions. For the first set of fluctuations we had,

$$\delta\Phi = nf(r)h_k^{(1)}(r)\exp(-i(n-k)\theta), \tag{8.25}$$

$$\delta A_1 = -\left(\frac{dh_k^{(1)}}{dr} + \frac{k}{r}h_k^{(1)}\right)\sin((k-1)\theta), \tag{8.26}$$

$$\delta A_2 = -\left(\frac{dh_k^{(1)}}{dr} + \frac{k}{r}h_k^{(1)}\right)\cos((k-1)\theta). \tag{8.27}$$

The second set of fluctuations were of the form,

$$\delta\Phi = -inf(r)h_k^{(2)}(r)\exp(-i(n-k)\theta), \tag{8.28}$$

$$\delta A_1 = \left(\frac{dh_k^{(2)}}{dr} + \frac{k}{r}h_k^{(2)}\right)\cos((k-1)\theta), \tag{8.29}$$

$$\delta A_2 = -\left(\frac{dh_k^{(2)}}{dr} + \frac{k}{r}h_k^{(2)}\right)\sin((k-1)\theta). \tag{8.30}$$

The interesting scattering process with $\frac{\pi}{n}$ symmetry occured when $k = n$, which was the one we studied in detail in the text. We formulated an initial value problem with the Euler-Lagrange equations. We supplemented this using the gauge condition,

$$\partial_\mu a^\mu = 0, \tag{8.31}$$

which ensures uniqueness of the solution for all time. We checked that the initial data chosen satisfied the conditions of [19]. The Gauss law and the Lorentz condition hold at $t = 0$. It is shown in [19] that they propagate. The initial value problem was restated as an integral equation,

$$\Psi(t, \vec{x}) = e^{-i\tilde{A}t}\Psi(0, \vec{x}) + \int_0^t ds \exp[-i\tilde{A}(t-s)]J(\Psi(s, \vec{x})), \tag{8.32}$$

and solved by an iterative method. It has been shown that this integral equation defines a contraction mapping. We used it to show that symmetries of the initial data are retained on iteration and so are exhibited in the solution. We examined the symmetries of solutions which are initially as symmetric as possible. At times $t > 0$, there are n vortices equidistant from the origin. They are directed with equal energies towards the origin, with relative angular separations $\frac{2\pi}{n}$. In this scattering process the radial directions along which the vortices leave after scattering are rotated relative to the incident angles by an angle $\frac{\pi}{n}$.

We examined to a lesser extent other scattering processes. In [18] and [24] it is stated that the $2n$ zero modes may be used to place the vortices at arbitrary points in plane. In the last chapter we used this property to try and create other interesting scattering processes. We used an approximation to the modulus of the Higgs field,

$$|\Phi|^2 = f^2(1 + \alpha n(h(r,\theta) + h^*(r,\theta)) + \alpha^2 n^2 |h(r,\theta)|^2) \tag{8.33}$$

to locate the vortices at chosen positions, which are its local minima. This allowed us to set up scattering processes with zeroes of the Higgs field moving in arbitrary predetermined directions.

In the first half of the thesis, in various models, the conditions for the existence of extended objects were studied. In the second half, we have shown for one of the models how we could build on our knowledge of static solutions and describe some of the dynamics of these extended objects.

Bibliography

[1] V.L. Ginzburg and L.D. Landau,
Zh. Eksp. Theor. Fiz **20** (1950) 1064.

[2] L. Jacobs, A. Khare, C. N. Kumar, and S. Paul,
Int. J. Mod. Phys. **A6** (1991) 3441.

[3] G. t'Hooft, Nucl. Phys. **B79** (1974) 276.

[4] A.M. Polyakov, JETP Lett. **20** (1974) 194.

[5] N.S. Manton, Phys. Lett. **B110** (1982) 54.

[6] D. Stuart, Comm. Math. Phys. **159** (1994) 51.

[7] D. Stuart, Comm. Math. Phys. **166** (1995) 149.

[8] A. Kudryavtsev, B. Piette and W.J. Zakrzewski, Phys. Lett. **A180** (1993) 119.

[9] J. Dziarmaga, Phys. Rev. **D49** (1994) 5609.

[10] N.S. Manton and M.K. Murray, Nonlinearity **8** (1995) 661.

[11] B.J. Schroers, Phys. Lett. **B356** (1995) 291.

[12] L. Jacobs and C. Rebbi, Phys. Rev. **B19** (1979) 4486.

[13] K. Arthur, Phys. Lett. **B356** (1995) 509.

[14] K. Arthur, D.H. Tchrakian and Y. Yang, Phys. Rev. **D** To appear.

[15] J. Gladikowski,University of Durham preprint, DTP 95-75.

[16] J. Hong, Y. Kim, P.Y. Pac, Phys. Rev. Lett. **64** (1990) 2230.

[17] R. Jackiw and E. Weinberg, Phys. Rev. Lett. **64** (1990) 2234.

[18] E.J Weinberg, Phys. Rev. **D19** (1979) 3008.

[19] J. Burzlaff and V. Moncrief, J. Math. Phys. **26** (1985) 1368.

[20] B.J. Plohr, Doctoral Dissertation, Princeton University (1980); J. Math. Phys. **22** (1981) 2184.

[21] K. Arthur and J. Burzlaff, Lett. in Math. Phys. **36** (1996) 311.

[22] I.G. Petrovsky, *Lectures on Partial Differential Equations*, Interscience, New York, 1954.

[23] F. Abdelwahid and J. Burzlaff, J. Math. Phys. **35** (1994)4651.

[24] A. Jaffe and C. Taubes, *Vortices and Monopoles*, Birkhäuser, Boston, 1980.

[25] William H. Press, *Numerical Recipes in C*, Cambridge University Press, 1992.